AD-A050 285 YALE UNIV NEW HAVEN CONN DEPT OF ENGINEERING AND AP--ETC F/G 17/1
SIGNAL PROCESSING FOR VERY LARGE ARRAYS.(U)
JUN 76 P M SCHULTHEISS, S CHOW N66001-75-C-0210

UNCLASSIFIED NL

| OF |
AD A050285

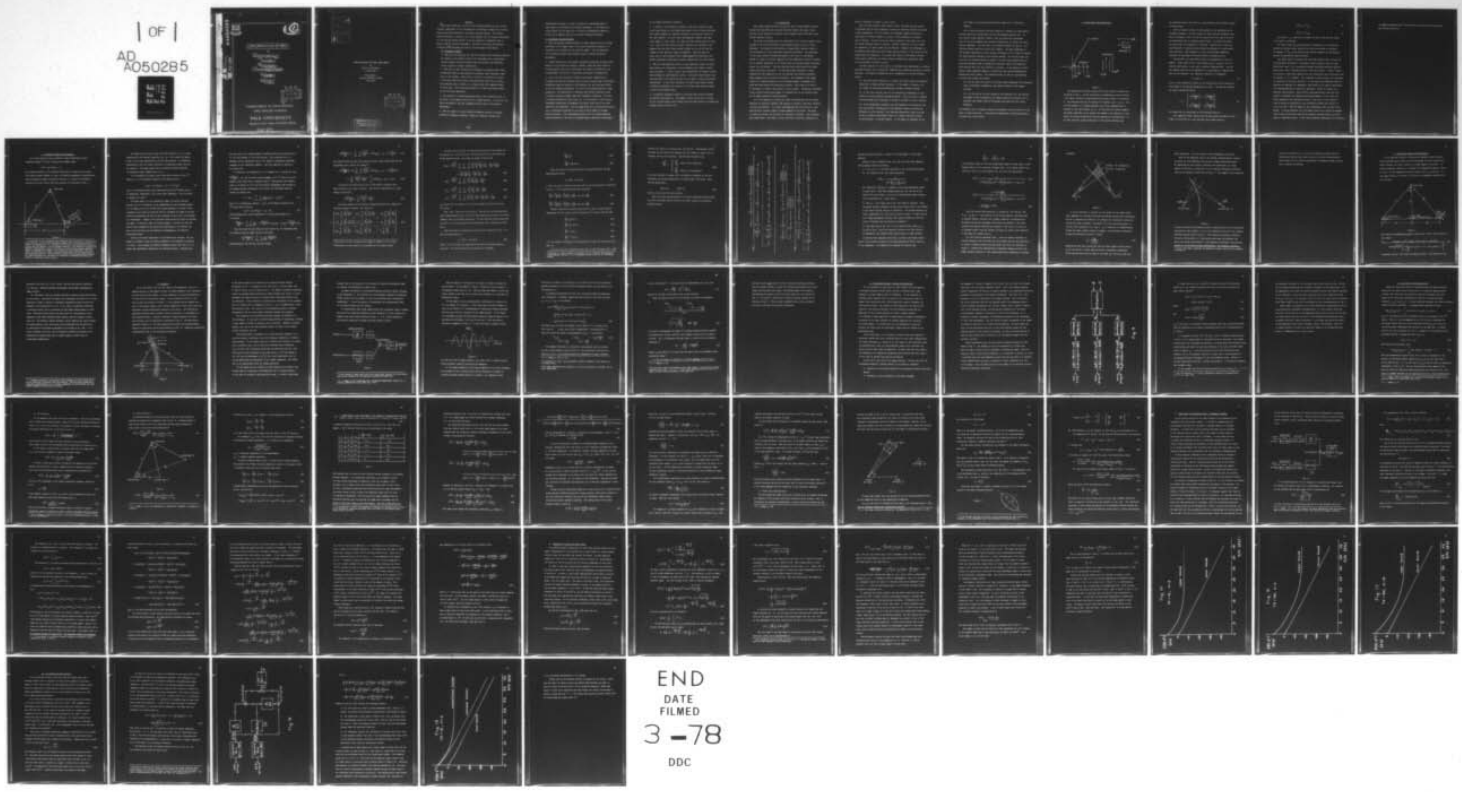

END
DATE FILMED
3-78
DDC

(1)

(6) SIGNAL PROCESSING FOR VERY LARGE ARRAYS.

BY

(10) Peter M./Schultheiss
Siu-Kay/Chow

(9) Final Report.,

(15) Contract N66001-75-C-0210

(11) June 1976

(12) 74p.

DEPARTMENT OF ENGINEERING
AND APPLIED SCIENCE

YALE UNIVERSITY

400 987

IV

SIGNAL PROCESSING FOR VERY LARGE ARRAYS

by

Peter M. Schultheiss

Siu-Kay Chow

Final Report

Contract N66001-75-C-0210

June 1976

Abstract

This report deals with the use of many sensors grouped into two or more clusters (subarrays) for the determination of bearing and range to an acoustic source producing sinusoidal or narrowband Gaussian signals. The spacing between subarrays is typically very large compared with the acoustic wavelength, but the spacing between sensors in any one subarray is comparable with or smaller than the acoustic wavelength. The noise is Gaussian and spatially incoherent. The following are some of the more general conclusions.

A. Sinusoidal signals

1. When only two subarrays are used the estimator which optimally combines the outputs of all sensors offers little advantage over a system which obtains separate bearing estimates from each subarray and determines source location by simple triangulation.

2. When three or more subarrays are available an estimator which forms conventional beams at each subarray and combines these coherently comes close to the optimum. Hence there is little or no incentive to build a much more complicated system using individual sensor data as inputs. Each subarray acts, in effect, as a single sensor with improved signal to noise ratio. The directional properties of these equivalent sensors are of only minor importance.

3. The accuracy of a system employing three or more subarrays could, in principle, be far greater than that of a single subarray. In practice, the factor discussed in the next paragraph severly limits this potential improvement.

4. When the signal is a pure sinusoid estimation accuracy is limited primarily by ambiguity problems. These are caused by the fact that

differential distances to a pair of sensors are indistinguishable if they differ by a multiple of the signal wavelength. In the absence of source motion the only good way to resolve such ambiguities appears to be the use of signals which are not single frequency sinusoids.

B. Narrowband Gaussian Signals

1. When the spacing between subarrays is large compared with the average wavelength of the signal, most of the useful information appears to be contained in the envelope of the received signal. Only the envelopes of the subarray outputs were therefore used in coherent estimation procedures.

2. Formal evaluation of the optimal estimator working with envelope information is a very difficult problem. However, lower and upper bounds on its mean square error can be calculated, the former by working with the pre-envelopes, the latter by evaluating a particular instrumentation.

3. One of the key questions is whether the coherent combination of envelopes from several subarrays yields a better estimate than conventional procedures using the sensors in only subarray, but now utilizing carrier as well as sideband information. The answer is straightforward for range estimation: The combination of envelopes from several subarrays yields a far more accurate estimate under most reasonable conditions. The case of bearing estimation is less clear cut. It is possible to find entirely reasonable combinations of parameters for which either one or the other scheme will be preferable. For the single array the far field bearing accuracy is determined primarily by the ratio of array length to average signal wavelength. The corresponding quantity for the system employing several subarrays is the ratio of spacing between subarrays to wavelength

of the highest modulation frequency.

4. A version of the ordinary (2 element) split beam tracker was used to set upper bounds on the minimum mean square error in delay estimation. This tracker employs the squared envelopes of two subarray outputs as its input signals. For very large time-bandwidth products and large input signal to noise ratios, the upper and lower bounds differ by about 6 db. Since the lower bound is almost certainly not realizable, this suggests that the split beam envelope tracker is not too far from the optimum in this important range of parameters. When the signal to noise ratio at each subarray (after beamforming) falls below unity the tracker performance deteriorates rapidly compared with the lower bound.

5. When the time-bandwidth product is only moderately large, the split beam tracker error approaches a finite minimum as the signal to noise ratio increases. It comes close to this minimum when the signal to noise ratio exceeds the time-bandwidth product. The lower bound predicts that the mean square error approaches zero as the signal to noise ratio grows indefinitely. In this case, therefore, the split beam tracker suffers a definite performance loss relative to the lower bound when the signal to noise ratio becomes large.

6. An improved (balanced) version of the split beam tracker overcomes the problem mentioned in 5. For signal to noise ratios well in excess of 0 db its mean square error differs from the lower bound by an essentially constant factor of about 6 db.

1. Introduction

This report summarizes work carried out under contract N66001-75-C-0210 between Yale University and the Naval Undersea Center, San Diego. Major portions of the material are adapted from a progress report and three letter reports submitted earlier.

The study is concerned with the localization of an acoustic signal source by means of an array consisting of many sensors grouped into two or more subarrays. The acoustic source radiates a signal which consists either of pure sinusoids or of very narrowband noise-like waveshapes. The wavelength of the signal sinusoid (average wavelength in the case of a narrowband signal) is likely to be small compared with the dimensions of any one subarray but is probably comparable to (or larger than) the spacing between individual sensors in the subarray. Thus the subarrays have beam patterns with significant directional properties. The spacing between subarrays is large compared with the dimensions of any one subarray and therefore extremely large compared with the acoustic wavelength. The frequency of the signal sinusoid (or center-frequency of the narrowband signal) is assumed to be known and fixed during the observation interval. Thus there is no effort to determine, or exploit, any effects of source motion. Information concerning source location (bearing and range) is contained only in the relative delay of the signal observed at various sensors.

All of the analysis is carried out under the assumption that the signal wavefront is perfectly coherent from subarray to subarray (and hence certainly over any one subarray). To a first approximation one could think of a less than perfectly coherent signal as being composed of two parts: One which is perfectly coherent and one which is completely incoherent. The incoherent part simply adds to the noise, so that the effect of partial incoherence is

merely a reduction in signal to noise ratio.

Only the most primitive noise model is used: The noise at each sensor is Gaussian, and the noise components received by different sensors are statistically independent. For the analysis of sinusoidal signals the noise at each sensor is further assumed to be white. This assumption is probably quite realistic: Practical sea noise spectra should be very nearly flat over the narrow frequency bands of interest. Spatial incoherence is a more doubtful assumption, at least within any one subarray. However, the advantages to be gained by exploiting such short range spatial structure of the noise are both limited and well understood. To include this effect in the present analysis would greatly complicate the results without shedding much additional light on the questions of primary interest.

The basic objective of the study is to determine what improvements in bearing and range accuracy can be obtained by combining the information supplied by various subarrays. The required combination can be accomplished at several different levels:

(1) The most general approach is to regard all sensor outputs as potential inputs into a single optimal estimator. If the number of sensors is at all large, the resulting instrumentation becomes extremely complex.

(2) At the other extreme, one can use conventional beamforming at each subarray to obtain separate bearing estimates. These can then be combined by purely geometrical techniques to obtain an estimate of source location.

(3) As an intermediate procedure, one can beamform at each subarray, and then use coherent combinations of the beamformer outputs to obtain the estimate of source location. This approach effectively treats each subarray as a single (directional) sensor in a larger array whose output is now processed in optimal fashion. If the number of subarrays is not

very large, the resulting instrumentation might not be excessively complex.

All of these procedures have been studied to a greater or lesser extent. We shall begin this presentation with the most general approach (1). It will quickly become apparent, however, that its theoretical advantages over (3) are quite marginal and certainly insufficient to justify the vastly greater complexity. The real choice is therefore between (2) and (3). The decision between these two is much less clearcut. The major advantage of the coherent combination of array outputs envisioned in (3) is that it exploits the large baseline provided by the subarray spacing. On the other hand, the fact that the subarray spacing is likely to be very large compared with the acoustic wavelength leads to ambiguities (multiple lobes in the effective beam pattern) which are very difficult to resolve. In the absence of source motion, signal bandwidth appears to furnish the only visible mechanism for dealing with this problem. The tradeoff between (2) and (3) can therefore be stated very roughly as follows:

(a) One can work with arrays of relatively small dimensions (the subarrays) using a wavelength determined by the center frequency of the signal spectrum.

(b) One can exploit the full spacing of the subarrays, but the relevant wavelength is now determined by the highest modulation frequency and is therefore much larger than the wavelength associated with the center frequency.

For different sets of parameter values the advantage can shift from one to the other of these procedures. A more detailed examination of these questions is a primary aim of this report.

2. Basic Theory and Definitions

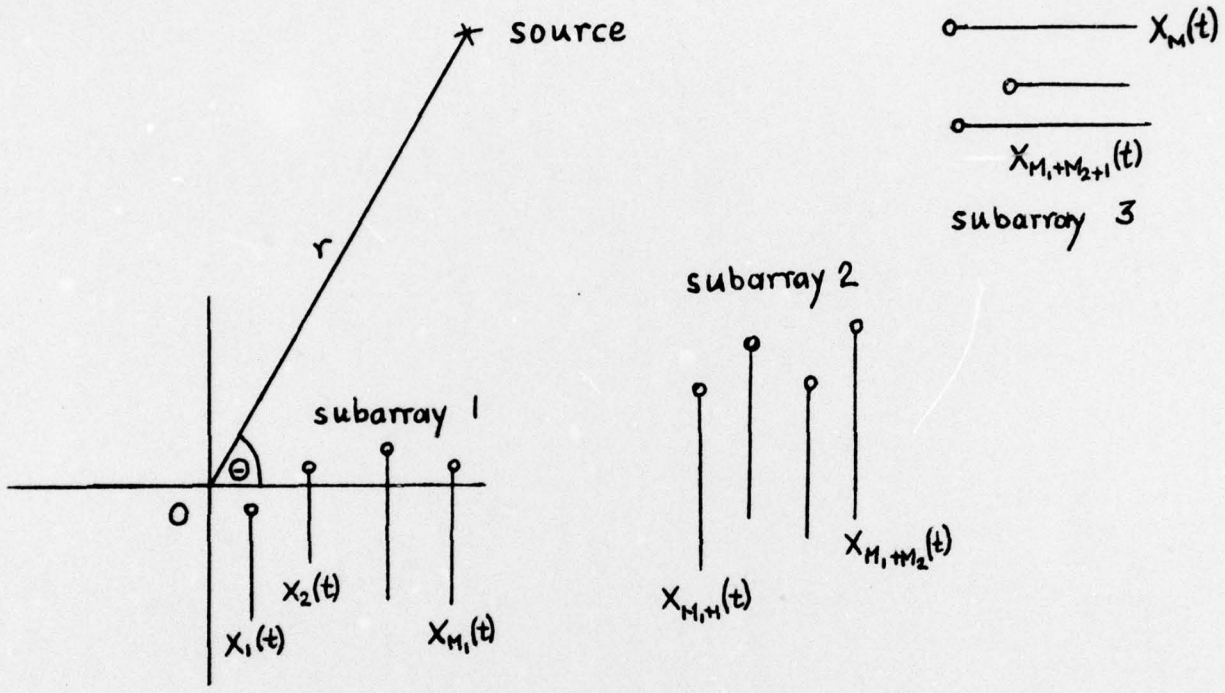

Figure 1

The geometrical relations between source and receiver locations are indicated in Fig. 1. We are interested in estimating the source bearing θ and range r relative to some conveniently chosen origin of coordinates 0. The available data are the outputs of M sensors, $x_1(t)...x_M(t)$. Each of these consists of a signal component and a noise component and is observed in the time interval (0, T). In line with the earlier comments the signal components at all sensors are assumed to be identical in form except for delays determined by strictly geometrical considerations. We do allow different signal attenations to the various subarrays and

can therefore discuss the effect of using subarrays with different signal to noise ratios.

There is always a degree of arbitrariness in the definition of an "optimum" estimator. We shall require at least that the estimator introduce no systematic error, so that the actual error will tend to zero as the observation time T increases without bound. In statistical terms, we require that our estimator be "unbiased". Beyond that, we take the usual approach of characterizing estimator performance by a mean square error criterion. This enables us to use the well-known Cramèr-Rao technique for obtaining the desired bounds on estimation error.

Specifically, let each sensor output be represented by a set of n numbers. These might be the n time samples $x_i(t_1)...x_i(t_n)$, a set of n Fourier coefficients, or any other convenient representation. Let $\underline{x}$ be the complete data vector of dimension M·n, consisting of n samples from each of the M sensors. The likelihood function Λ is defined by

$$\Lambda = p(\underline{x} | \theta, r) \tag{1}$$

Thus Λ is the probability density of the received data vector $\underline{x}$ when the true values of the unknown parameters are θ and r. We must now evaluate the Fisher information matrix

$$J = - \begin{bmatrix} E\left\{\frac{\partial^2 \log \Lambda}{\partial \theta^2}\right\} & E\left\{\frac{\partial^2 \log \Lambda}{\partial \theta \partial r}\right\} \\ E\left\{\frac{\partial^2 \log \Lambda}{\partial r \partial \theta}\right\} & E\left\{\frac{\partial^2 \log \Lambda}{\partial r^2}\right\} \end{bmatrix} \tag{2}$$

E{} stands for the expectation of the bracketed quantity.

The Cramèr-Rao theory asserts that the mean square estimation errors $D^2(\hat{\theta})$ of θ and $D^2(\hat{r})$ of r have absolute lower bounds given by

$$D^2(\hat{\theta}) \geq [J^{-1}]_{11} \tag{3}$$

$$D^2(\hat{r}) \geq [J^{-1}]_{22} \tag{4}$$

The symbol $[\ ]_{ij}$ indicates the element in the ith row and jth column of the matrix in brackets.

The lower bounds are entirely general, independent of the particular estimation procedure used, assuming only that the estimate is unbiased. The element $[J^{-1}]_{12}$ of the inverse Fisher matrix measures the correlation between the bearing and range estimates.

One cannot assert in general that the lower bounds of Eqs. (3) and (4) are necessarily attainable. The general theory indicates that for large observation times T, the (realizable) maximum likelihood estimator achieves mean square errors approaching those of the lower bounds. "Large T" means, in practice, a time large compared with the correlation time of the noise (and the signal, if it is random). This condition is quite likely to be satisfied in situations of practical interest. In this sense the Cramèr-Rao bound can therefore be regarded as a meaningful limit which can at least be approached with instrumentations of sufficient complexity. There is, however, one important qualification: Most practical instrumentations, even when they purport to implement the maximum likelihood estimator, do not locate the global maximum of the likelihood function. They find a local maximum, a point at which the derivative of the likelihood function with respect to θ and r is zero. When the signal is very narrowband, there are many local maxima. In using Cramèr-Rao as a realizable bound we are therefore assuming that we have successfully resolved the ambiguity problem posed by multiple peaks of comparable height. As the signal bandwidth diminishes, the difference

in height of adjacent peaks decreases and the resolution problem becomes more and more difficult.

3. Sinusoidal Signal, Two Subarrays

As a first specific case we consider a source radiating a purely sinusoidal signal [1] of known frequency but unknown phase

$$s(t) = A_0 \sin(\omega_0 t - \phi). \tag{5}$$

The receiver consists of two subarrays which will be taken as line arrays with equally spaced elements in order to simplify trigonometric manipulations. Source bearing and range are measured relative to a system of coordinates centered at the left end of the first subarray, as indicated in Fig. 2.

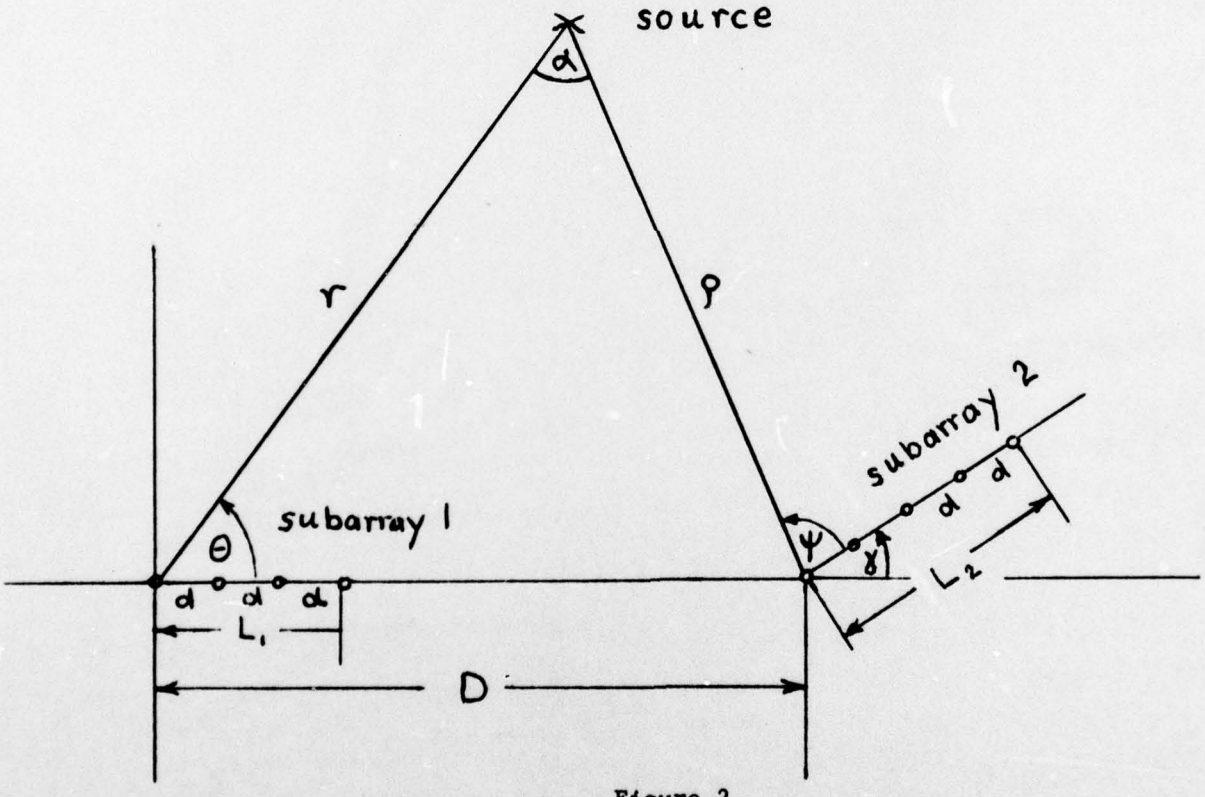

Figure 2.

[1] In the light of the discussion just completed this problem has a rather artificial flavor. With a purely sinusoidal signal there is no practical way to resolve the ambiguities. To calculate how accurate a system would be which did resolve them may appear to be an academic exercise. The reason for pursuing the argument nevertheless is that it exhibits in a particularly simple setting a number of problems which remain, but become much less transparent, when the signal is sufficiently complex to permit identification of the global peak in the likelihood function. These problems include the coupling between bearing and range estimation and the merits of coherently combining beam outputs as opposed to individual sensor outputs.

We assume that the source range from each subarray (r, ρ) is large compared with the subarray dimensions (L_1, L_2). As a result the angles θ and ψ do not vary significantly over any one subarray. An equivalent observation is that the signal wavefront is essentially planar over any one subarray. We do not assume that the spacing D between subarrays is necessarily small compared with r or ρ.

If we designate the signal travel time from the source to the i^{th} sensor by τ_i, the waveshape received at that sensor will be

$$x_i(t) = A_i \sin[\omega_0(t - \tau_i) - \phi] + n_i(t) \tag{6}$$

$n_i(t)$ is the Gaussian white noise associated with the i^{th} sensor and is, by assumption, independent of all other noise components. Only the delay τ_i depends on r and θ.

The phase angle ϕ of the transmitted signal is without intrinsic interest, but it is essential to the computation for the following reason: If ϕ is taken as zero (or as some other known quantity), the time of zero crossings at the source is known and one can determine the range to any one receiver by observing the time of zero crossings at that point (to multiples of a wavelength). Ranges to two receivers would locate the source in bearing and range. In practice, this is clearly nonsense. One does not know the time of zero crossings at the source and observations at two sensors can only locate the source on the hyperbola corresponding to the observed differential delay.

There are two basic approaches to the problem just outlined. One can regard ϕ as another fixed but unknown parameter to be estimated in addition to θ and r. This enlarges the Fisher information matrix [Eq. (2)] to 3 x 3 format and considerably complicates the inversion process. Alternatively

one can treat ϕ as a random parameter [perhaps uniformly distributed over $(0, 2\pi)$] and average over its distribution. This preserves the 2 x 2 dimension of the information matrix, but leads to exceedingly cumbersome integrals in its individual elements. The first approach is chosen as the lesser evil.

To illustrate the computation of the elements of J, consider the term $E[\frac{\partial^2 \log \Lambda}{\partial \theta^2}]$. We take the noise spectral level at the i^{th} sensor as N_i and assume a noise white over a frequency band W. Then Nyquist rate samples taken at intervals of 1/2 W are statistically independent and, because of the assumed spatial incoherence of the noise, the likelihood function assumes the simple form

$$\Lambda = C \exp \{- \sum_{i=1}^{M} \sum_{j=1}^{n} \frac{1}{2N_i W}[x_i(t_j) - s_i(t_j)]^2\} \tag{7}$$

where C is a normalizing constant. $s_i(t)$ is the signal received at the i^{th} sensor and is given by

$$s_i(t) = A_i \sin[\omega_0(t - \tau_i) - \phi]. \tag{8}$$

Differentiating the natural logarithm of (7) twice with respect to θ one obtains

$$\frac{\partial^2 \log \Lambda}{\partial \theta^2} = \sum_{i=1}^{M} \sum_{j=1}^{n} \frac{1}{N_i W} \{ - [\frac{\partial s_i(t_j)}{\partial \theta}]^2 + [x_i(t_j) - s_i(t_j)] \frac{\partial^2 s_i(t_j)}{\partial \theta^2}\}. \tag{9}$$

Since the noise has zero mean the last term in Eq. (9) disappears when the expected value is taken and one is left with

$$-E\left\{\frac{\partial^2 \log \Lambda}{\partial \theta^2}\right\} = \sum_{i=1}^{M} \sum_{j=1}^{n} \frac{1}{N_i W} [\frac{\partial s_i(t_j)}{\partial \theta}]^2 \tag{10}$$

Substituting Eq. (8) into Eq. (10) one obtains

$$- E\left[\frac{\partial^2 \log \Lambda}{\partial \theta^2}\right] = \sum_{i=1}^{M} \sum_{j=1}^{n} \frac{A_i^2 \omega_0^2}{N_i W} \cos^2[\omega_0(t_j - \tau_i) - \phi] \left(\frac{\partial \tau_i}{\partial \theta}\right)^2. \qquad (11)$$

For large W there are many time samples in each signal period and one can approximate the j sum by an integral.[1]

$$- E\left[\frac{\partial^2 \log \Lambda}{\partial \theta^2}\right] = 2W \sum_{j=1}^{n} \left\{ \sum_{i=1}^{M} \frac{A_i^2 \omega_0^2}{N_i W} \cos^2[\omega_0(t_j - \tau_i) - \phi] \left(\frac{\partial \tau_i}{\partial \theta}\right)^2 \right\} \Delta t$$

$$\simeq 2 \sum_{i=1}^{M} \frac{A_i^2 \omega_0^2}{N_i} \left(\frac{\partial \tau_i}{\partial \theta}\right)^2 \int_0^T \cos^2[\omega_0(t - \tau_i) - \phi] \, dt. \qquad (12)$$

In practice the observation time T would almost certainly cover many periods of the signal sinusoid. Then one can approximate to a high degree of accuracy[2]

$$- E\left[\frac{\partial^2 \log \Lambda}{\partial \theta^2}\right] \simeq \sum_{i=1}^{M} \frac{A_i^2 \omega_0^2 T}{N_i} \left(\frac{\partial \tau_i}{\partial \theta}\right)^2. \qquad (13)$$

The other elements of the Fisher information matrix are computed in entirely analogous fashion. The result is

$$J = \left[\begin{array}{c|c|c} \omega_0^2 T \sum_{i=1}^{M} \frac{A_i^2}{N_i} \left(\frac{\partial \tau_i}{\partial \theta}\right)^2 & \omega_0^2 T \sum_{j=1}^{M} \frac{A_i^2}{N_i} \frac{\partial \tau_i}{\partial \theta} \frac{\partial \tau_i}{\partial r} & \omega_0 T \sum_{i=1}^{M} \frac{A_i^2}{N_i} \frac{\partial \tau_i}{\partial \theta} \\ \hline \omega_0^2 T \sum_{i=1}^{M} \frac{A_i^2}{N_i} \frac{\partial \tau_i}{\partial \theta} \frac{\partial \tau_i}{\partial r} & \omega_0^2 T \sum_{i=1}^{M} \frac{A_i^2}{N_i} \left(\frac{\partial \tau_i}{\partial r}\right)^2 & \omega_0 T \sum_{i=1}^{M} \frac{A_i^2}{N_i} \frac{\partial \tau_i}{\partial r} \\ \hline \omega_0 T \sum_{i=1}^{M} \frac{A_i^2}{N_i} \frac{\partial \tau_i}{\partial \theta} & \omega_0 T \sum_{i=1}^{M} \frac{A_i^2}{N_i} \frac{\partial \tau_i}{\partial r} & T \sum_{i=1}^{M} \frac{A_i^2}{N_i} \end{array}\right] \qquad (14)$$

---

[1] Note that the time increment from sample to sample is $\Delta t = 1/(2W)$.

[2] The result is exact when T is a multiple of the signal period.

A tedious but basically straightforward computation now yields the determinant of J and the various cofactors required for the evaluation of the inverse matrix. The terms of primary interest are

$$\text{Det } J = \frac{\omega_0^4 T^3}{2} \sum_{i=1}^{M} \sum_{j=1}^{M} \sum_{k=1}^{M} \frac{A_i^2}{N_i} \frac{A_j^2}{N_j} \frac{A_k^2}{N_k} \left\{ \left(\frac{\partial \tau_j}{\partial r} - \frac{\partial \tau_k}{\partial r} \right)^2 \left(\frac{\partial \tau_i}{\partial \theta} \right)^2 \right.$$

$$\left. - 2 \frac{\partial \tau_i}{\partial \theta} \frac{\partial \tau_j}{\partial \theta} \left(\frac{\partial \tau_i}{\partial r} - \frac{\partial \tau_k}{\partial r} \right) \left(\frac{\partial \tau_j}{\partial r} - \frac{\partial \tau_k}{\partial r} \right) \right\} \tag{15}$$

$$J_{11} = \frac{\omega_0^2 T^2}{2} \sum_{j=1}^{M} \sum_{k=1}^{M} \frac{A_j^2}{N_j} \frac{A_k^2}{N_k} \left(\frac{\partial \tau_j}{\partial \theta_r} - \frac{\partial \tau_k}{\partial \theta_r} \right)^2 \tag{16}$$

$$J_{22} = \frac{\omega_0^2 T^2}{2} \sum_{j=1}^{M} \sum_{k=1}^{M} \frac{A_j^2}{N_j} \frac{A_k^2}{N_k} \left(\frac{\partial \tau_j}{\partial \theta} - \frac{\partial \tau_k}{\partial \theta} \right)^2 \tag{17}$$

$$J_{12} = \frac{\omega_0^2 T^2}{2} \sum_{j=1}^{M} \sum_{k=1}^{M} \frac{A_j^2}{N_j} \frac{A_k^2}{N_k} \left(\frac{\partial \tau_j}{\partial \theta} - \frac{\partial \tau_k}{\partial \theta} \right) \left(\frac{\partial \tau_j}{\partial r} - \frac{\partial \tau_k}{\partial r} \right) \tag{18}$$

$J_{r\ell}$ stands for the cofactor of the matrix element in the rth row and ℓth column.

Eqs. (15) - (18) are quite general. They do not use the particular array configuration of Fig. 2, nor do they require the source to be remote compared with the subarray dimensions. We now introduce these assumptions in order to put the various partial derivatives into a relatively simple form.

When the index j is associated with the first subarray in Fig. 2 we have the approximation

$$\tau_j = \frac{1}{c} (r - jd \cos \theta) \tag{19}$$

where c is the velocity of sound and d the distance between adjacent elements. The required partial derivatives are therefore

$$\frac{\partial \tau_j}{\partial r} = \frac{1}{c} \tag{20}$$

$$\frac{\partial \tau_j}{\partial \theta} = j \frac{d}{c} \sin \theta \tag{21}$$

When the index k is associated with the second subarray the same approximation yields

$$\tau_k = \frac{1}{c}(\rho - kd \cos \psi) \tag{22}$$

ρ and ψ are source range and bearing from the second subarray as indicated in Fig. 2. The required partials are therefore

$$\frac{\partial \tau_k}{\partial r} = \frac{\partial \tau_k}{\partial \rho} \frac{\partial \rho}{\partial r} + \frac{\partial \tau_k}{\partial \psi} \frac{\partial \psi}{\partial r} = \frac{1}{c}(\frac{\partial \rho}{\partial r} + kd \sin \psi \frac{\partial \psi}{\partial r}) \tag{23}$$

$$\frac{\partial \tau_k}{\partial \theta} = \frac{\partial \tau_k}{\partial \rho} \frac{\partial \rho}{\partial \theta} + \frac{\partial \tau_k}{\partial \psi} \frac{\partial \psi}{\partial \theta} = \frac{1}{c}(\frac{\partial \rho}{\partial \theta} + kd \sin \psi \frac{\partial \psi}{\partial \theta}) \ . \tag{24}$$

Simple trigonometric manipulations based on Fig. 2 yield explicit expressions for the various partial derivatives [1] in Eqs. (23) and (24)

$$\frac{\partial \psi}{\partial r} = \frac{1}{\rho} \sin \alpha \tag{25}$$

$$\frac{\partial \psi}{\partial \theta} = \frac{r}{\rho} \cos \alpha \tag{26}$$

$$\frac{\partial \rho}{\partial r} = \cos \alpha \tag{27}$$

$$\frac{\partial \rho}{\partial \theta} = r \sin \alpha \tag{28}$$

α is the angular separation of the subarrays as seen from the source [see Fig. 2].

The next step is to substitute Eqs. (23) - (28) into Eqs. (15) - (18)

[1] They are, of course, simply the elements of the Jacobian describing the transformation from the (r, θ) coordinate system to the (ρ, ψ) coordinate system.

and use the results to evaluate Eqs. (3) and (4). Considerable simplification can be achieved by assuming that the signal to noise ratio is constant over any one subarray. Specifically we shall write

$$\frac{A_i^2}{N_i} = \begin{cases} \dfrac{A_1^2}{N_1} & \text{when i is in subarray 1} \\ \dfrac{A_2^2}{N_2} & \text{when i is in subarray 2} \end{cases} \tag{29}$$

It is also helpful to assume that the numbers of elements in the two subarrays, M_1 and M_2 respectively, are much larger than unity. Then one can approximate

$$M_1 d = L_1, \qquad M_2 d = L_2 \tag{30}$$

where L_1 and L_2 are the array lengths.

Even with these approximations the required algebraic manipulations are still extremely tedious and only the final results are therefore reproduced here.

$$D^2(\hat{\theta}) \geq \frac{12(\cos\alpha - 1 + \frac{L_2}{2\rho}\sin\psi\sin\alpha)^2 + (\frac{L_2}{\rho}\sin\psi\sin\alpha)^2[1+\frac{(A_2^2/N_2)M_2}{(A_1^2/N_1)M_1}]}{4\pi^2T\left\{\frac{A_1^2}{N_1}M_1\frac{L_1^2}{\lambda^2}\sin^2\theta[(\cos\alpha - 1 + \frac{L_2}{2\rho}\sin\psi\sin\alpha)^2 + \frac{1}{12}(\frac{L_2}{\rho}\sin\psi\sin\alpha)^2] + \frac{A_2^2}{N_2}M_2\frac{L_2^2}{\lambda^2}\frac{r^2}{\rho^2}\sin^2\psi[(\cos^2\alpha - \sin^2\alpha - \cos\alpha + \frac{L_1}{2r}\sin\alpha\sin\theta)^2 + \frac{1}{12}(\frac{L_1}{r}\sin\alpha\sin\theta)^2]\right\}} \tag{31}$$

$$D^2(\hat{r}) \geq \frac{r^2\left\{12(\sin\alpha + \frac{L_2}{2\rho}\sin\psi\cos\alpha - \frac{L_1}{2r}\sin\theta)^2 + (\frac{L_1}{r}\sin\theta)^2[1+\frac{(A_1^2/N_1)M_1}{(A_2^2/N_2)M_2}] + (\frac{L_2}{\rho}\sin\psi\cos\alpha)^2[1+\frac{(A_2^2/N_2)M_2}{(A_1^2/N_1)M_1}]\right\}}{4\pi^2T^2\left\{\frac{A_1^2}{N_1}M_1\frac{L_1^2}{\lambda^2}\sin^2\theta[(\cos\alpha - 1 + \frac{L_2}{2\rho}\sin\psi\sin\alpha)^2 + \frac{1}{12}(\frac{L_2}{\rho}\sin\psi\sin\alpha)^2] + \frac{A_2^2}{N_2}M_2\frac{L_2^2}{\lambda^2}\frac{r^2}{\rho^2}\sin^2\psi[(\cos^2\alpha - \sin^2\alpha - \cos\alpha + \frac{L_1}{2r}\sin\alpha\sin\theta)^2 + \frac{1}{12}(\frac{L_1}{r}\sin\alpha\sin\theta)^2]\right\}} \tag{32}$$

The newly introduced symbol λ stands for the wavelength of the signal sinusoid.

Inspite of their complexity Eqs. (31) and (32) yield some immediate checks against physical intuition:

1) If $A_2 = 0$, i.e. the second subarray is not receiving any signal, Eq. (31) reduces to the very simple expression

$$D^2(\hat{\theta}) \geq \frac{12}{4\pi^2 T \frac{A_1^2}{N_1} M_1 \frac{L_1^2}{\lambda^2} \sin^2\theta} \tag{33}$$

The combination $A_1^2 M_1/N_1$ is a measure of the post-beamforming signal to noise ratio. With that interpretation Eq. (33) has all of the features one would expect to find in the minimum mean square bearing error attainable with a linear array.

2) When $A_1 \to 0$ the right side of Eq. (31) tends to infinity. This conclusion becomes reasonable as soon as one recalls that θ was defined as the source bearing relative to subarray 1. The second subarray provides a measurement of ψ which may be quite accurate. It does not permit a range measurement and hence does almost nothing to locate the source in bearing from the position of subarray 1.

3) The right side of Eq. (32) tends to infinity when either A_1 or A_2 tend to zero. Since the wavefront curvature over each subarray is negligible, one subarray alone cannot produce a range estimate.

In practice both subarrays would have to receive substantial signal levels if the overall system is to perform significantly better than one of its components. For simplicity we consider the special case

$$\frac{A_1^2}{N_1} M_1 = \frac{A_2^2}{N_2} M_2 \equiv W \frac{S}{N} \tag{34}$$

S/N therefore stands for the post-beamforming signal to noise ratio of each subarray and W is the processed frequency band. If we ignore terms of the order L_2/ρ and L_1/r we can simplify Eqs. (31) and (32) drastically:

$$D^2(\hat{\theta}) \geq \frac{12}{4\pi^2 TW \frac{S}{N} \left[\frac{L_1^2}{\lambda^2} \sin^2\theta + \frac{L_2^2}{\lambda^2}\frac{r^2}{\rho^2} \sin^2\psi(1 + 2\cos\alpha)^2\right]} \tag{35}$$

$$D^2(\hat{r}) \geq \frac{12\, r^2 \frac{1+\cos\alpha}{1-\cos\alpha}}{4\pi^2 TW \frac{S}{N} \left[\frac{L_1^2}{\lambda^2} \sin^2\theta + \frac{L_2^2}{\lambda^2}\frac{r^2}{\rho^2} \sin^2\psi(1 + 2\cos\alpha)^2\right]}$$

$$= \frac{1+\cos\alpha}{1-\cos\alpha}\, r^2 D^2(\hat{\theta}) \tag{36}$$

The first interesting comparison is between Eq. (35) and Eq. (33). If $L_1 \simeq L_2$ and $r \simeq \rho$ the addition of the second subarray, even when used in optimal fashion, produces only a modest reduction in bearing error. One gains the obvious advantages from having one subarray or the other oriented more nearly broadside with respect to the source, but there is no apparent benefit from the enormous increase in overall array dimension to the order of D rather than L_1.

Eq. (36) tells an analogous story. Given two similar subarrays at similar distances from the source one could simply use each one separately to obtain a bearing estimate and then locate the source as indicated in Figure 3. Treating the subarray outputs coherently appears to yield only modest benefits relative to this simple geometrical combination of bearing

estimates.

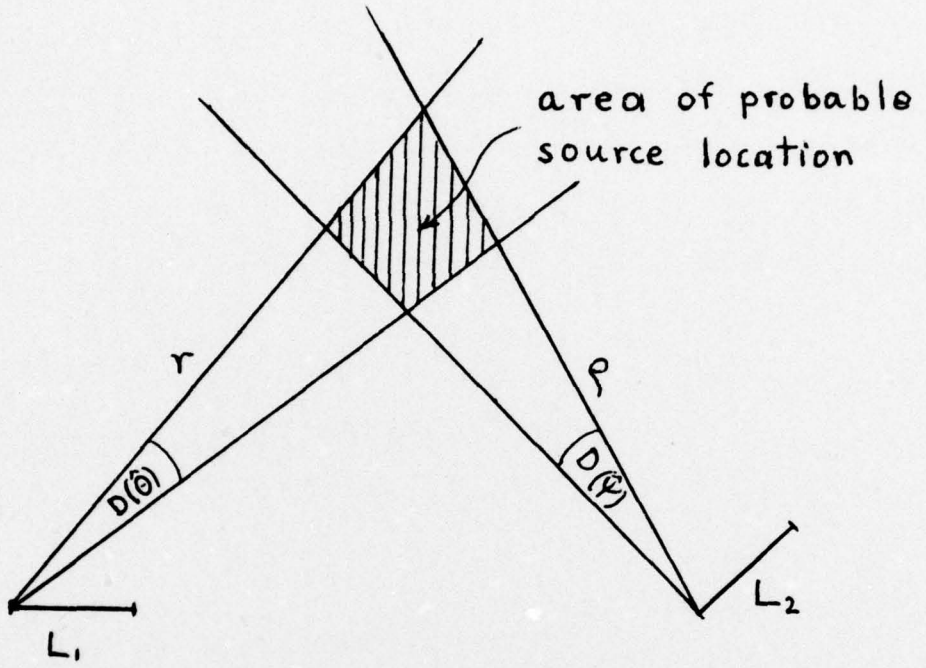

Figure 3.

It is not difficult to account for the failure of the large overall array dimension to influence the range and bearing accuracy more drastically. One way to approach the problem is to consider the correlation between the bearing and range estimates. The matrix J^{-1} is the covariance matrix of the best joint estimate of θ, r and ϕ. It is therefore a straightforward, though once again tedious, matter to compute the correlation coefficient between the estimation errors of $\hat{\theta}$ and $\hat{r}$.

$$\rho_{\theta r} = \frac{J_{12}}{\sqrt{J_{11} J_{22}}} \tag{37}$$

Computations have been carried out only for equal signal to noise ratios at the two arrays, in which case one finds a correlation coefficient differing from unity only by terms of the order L_1/r and L_2/ρ, both very

small quantities. One can interpret these observations as follows:

Each of the subarrays, even in the optimal instrumentation, produces an effect not very different from that of a single directional sensor. By combining the array outputs coherently one establishes, to a high degree of precision, a hyperbolic locus of constant differential distance from the two subarrays (solid line in Fig. 4). The segment of the hyperbola

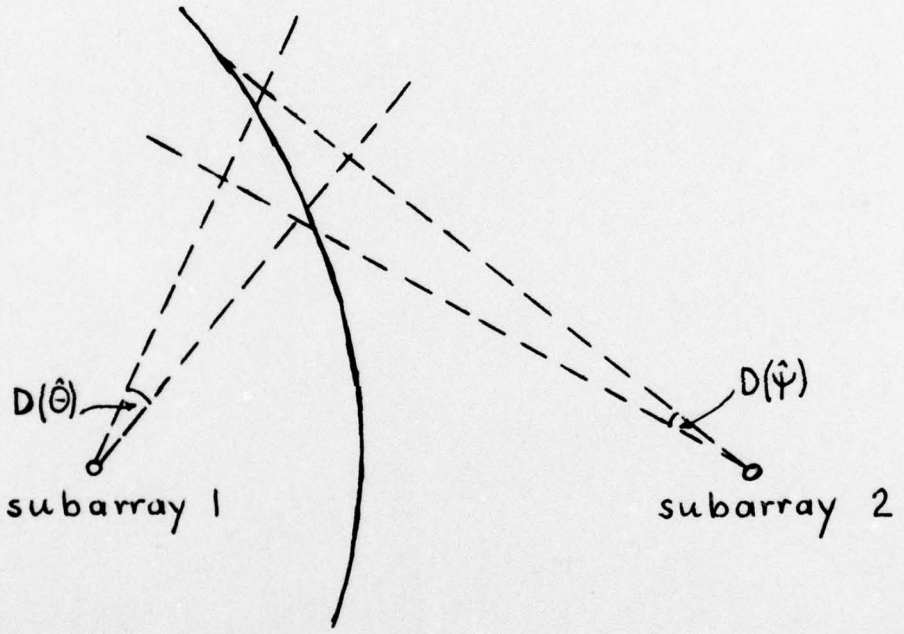

Figure 4

on which the source is actually located is identified only by the directional properties of each "sensor", i.e. by the estimation accuracy of the separate subarrays (dotted lines in Fig. 4). With coherent processing, therefore, the area of uncertainty is a very narrow strip along the hyperbola and within the dotted quadrilateral.[1] With separate processing of the subarray outputs it is the entire dotted quadrilateral. The hyperbola traverses,

[1] We are, once again, ignoring the ambiguity problem, which will be examined in section 5.

within the quadrilateral, a variety of bearing and range values not dramatically smaller than those covered by the entire quadrilateral. This accounts for the limited improvement in bearing and range accuracy due to coherent processing.

4. Sinusoidal Signal, Three Subarrays.

If two subarrays identify a hyperbola of probable source location, three subarrays should define two such hyperbolas and their intersection should pinpoint the source location to a high degree of precision. It appears promising, therefore, to examine the configuration shown in Fig. 5. As in Eq. (35) we immediately discard terms of order L_1/r and L_2/ρ. We also ignore terms of the order L_1/λ and L_2/λ as negligible compared with D_1/λ and D_2/λ.

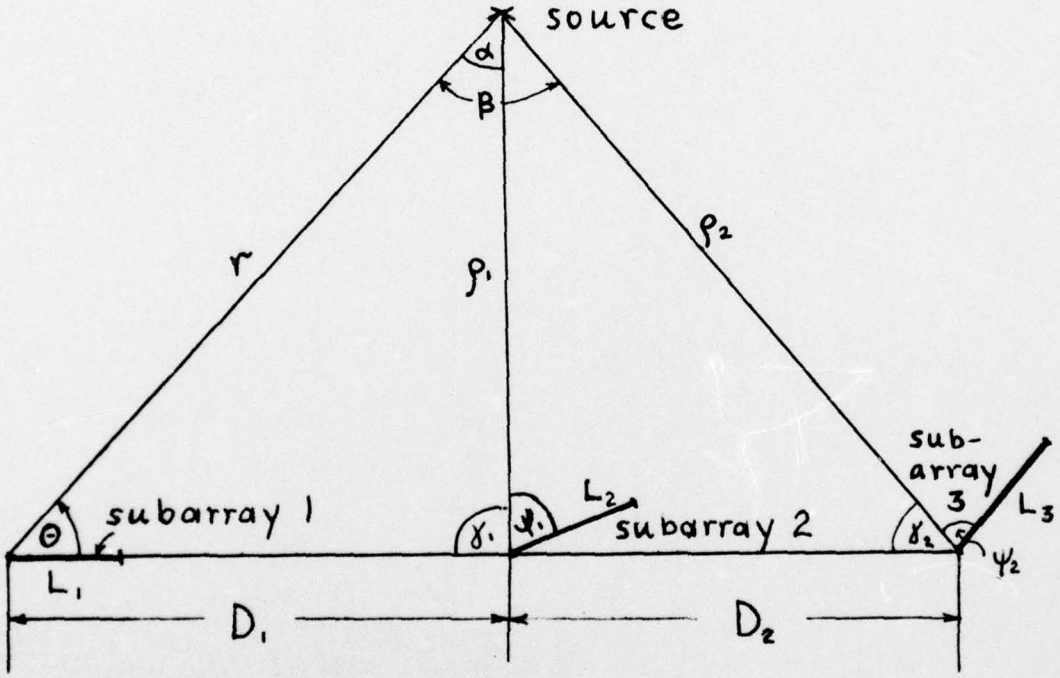

Figure 5.

With equal post-beamforming signal to noise ratio S/N at each subarray we then obtain

$$D^2(\hat{\theta}) \geq \frac{12[(\cos\alpha - 1)^2 + \cos(\beta - 1)^2 + (\cos\alpha - \cos\beta)^2]}{4\pi^2 TW \frac{S}{N}\left(\frac{D_1+D_2}{\lambda}\right)^2 \left[\frac{1}{1+\frac{D_2}{D_1}} \sin\gamma_1(\cos\alpha - 1) - \sin\gamma_2(\cos\beta - 1)\right]^2} \quad (38)$$

Comparison with Eq. (35) shows the expected result: The accuracy is now

governed by the ratio $(D_1 + D_2)/\lambda$ rather than the much smaller quantities L_1/λ and L_2/λ. Entirely parallel observations can be made concerning the range accuracy.

Eq. (38) goes a long way towards resolving a question raised much earlier in this report: How should one combine the information provided by the various subarrays in order to achieve a reasonable compromise between accuracy and complexity [see discussion on p. 2]? In Eq. (38) the subarrays contribute to bearing accuracy only by enhancing the post-beam forming signal to noise ratio. One would obtain exactly the same result by considering an array composed of only three omnidirectional sensors, each with signal to noise ratio S/N. The absolute optimum estimator, which combines all sensor outputs in optimal fashion, has a mean square error differing from the above only by terms which we discarded as negligible in arriving at Eq. (38). It is clear, therefore, that very little is gained by using the subarrays to do anything more sophisticated than to enhance signal to noise ratio by conventional beamforming.[1]

---

[1] It appears plausible to extrapolate this statement to noise fields which are not spatially incoherent over one subarray. One should now construct a reasonable approximation to the optimum beamformer for the subarray and then combine subarray contributions as before.

5. Ambiguity

All of our results thus far were based on the assumption that it is somehow possible to distinguish between the global maximum of the likelihood function and all other maxima. We have commented on the near-impossibility of doing this with sinusoidal signals. From a geometrical point of view one can pose the problem as follows: If two subarrays may be regarded as a pair of directional sensors, then a phase comparison at their output does not establish a unique differential distance to the source. All differential distances differing from a possible value by multiples of a wavelength are also possible values. Instead of defining a single hyperbola the sensor pair defines a set of hyperbolas as indicated in Fig. 6. The practically important question is: How many hyperbolas lie within the bearing-defined regions of uncertainty (dotted quadrilateral in Fig. 4)? Elementary geometrical considerations lead to the following conclusions:

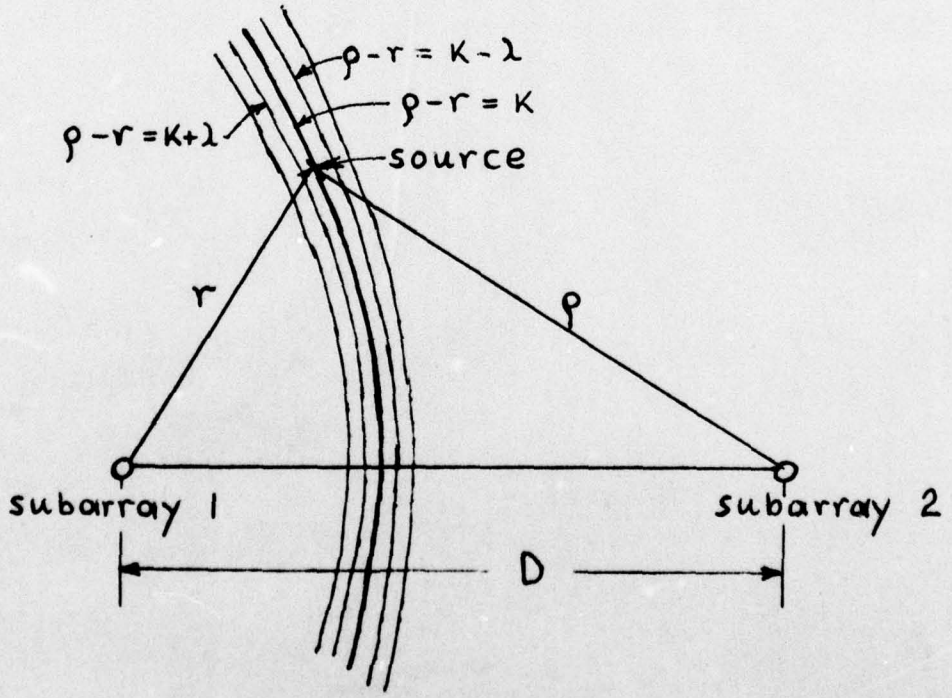

Figure 6

On the axis joining the two subarrays the distance between adjacent hyperbolas is $\lambda/2$. It remains of that order until r is much larger than D, then it begins to grow linearly with r. The number of possible hyperbolas within the bearing defined uncertainty region (shaded area of Fig. 3) would presumably be large and would not diminish with increasing distance from the subarrays. Source location is therefore not constrained to the neighborhood of a single line, as suggested by Fig. 4, but to neighborhoods of many near-parallel lines. The utility of the information gained by coherent processing of the two array outputs therefore becomes very marginal.

The situation is not improved materially through the addition of a third subarray. We now have two intersecting families of hyperbolas, yielding a large number of points as possible source locations. Ambiguity therefore appears to be one of the real limiting factors, at least in the problem setting considered thus far.

The obvious means of avoiding, or at least reducing, ambiguity is to work with signals containing two or more frequency components not harmonically related. If the signal consists of several pure sinusoids, the analysis of sections 3 and 4 can be used with relatively minor extensions. $s_1(t)$ is now a sum of sinusoids which must be substituted into Eq. (10). Since each of these sinusoids has the same delay τ_1, the only change in Eq. (13) will be replacement of $A_1^2\omega_0^2T$ by a more complicated term involving amplitudes and frequencies of all signal components. The remainder of the computations would not change materially.

If the signal does not consist of fixed sinusoids, but covers a continuous band of frequencies, the ambiguities can be resolved formally in the limit of extremely long observation times. In order to gain some

insight into the seriousness of the problem for realistic observation times we consider the following very simple case.

We model the signal as a narrowband Gaussian process of center frequency ω_0 and bandwidth $\Delta\omega$. The receivers are two subarrays, modelled as omnidirectional sensors with the signal to noise ratio achieved after conventional beamforming [1]. We are interested in determining the differentiated delay of the signal between the two sensors.

For observation times large compared with the correlation times of signal and noise this estimation problem is solved optimally [2] by the ordinary two element split beam tracker sketched in Fig. 7. H is a filter matched to the spectral properties of signal and noise (Eckart filter).

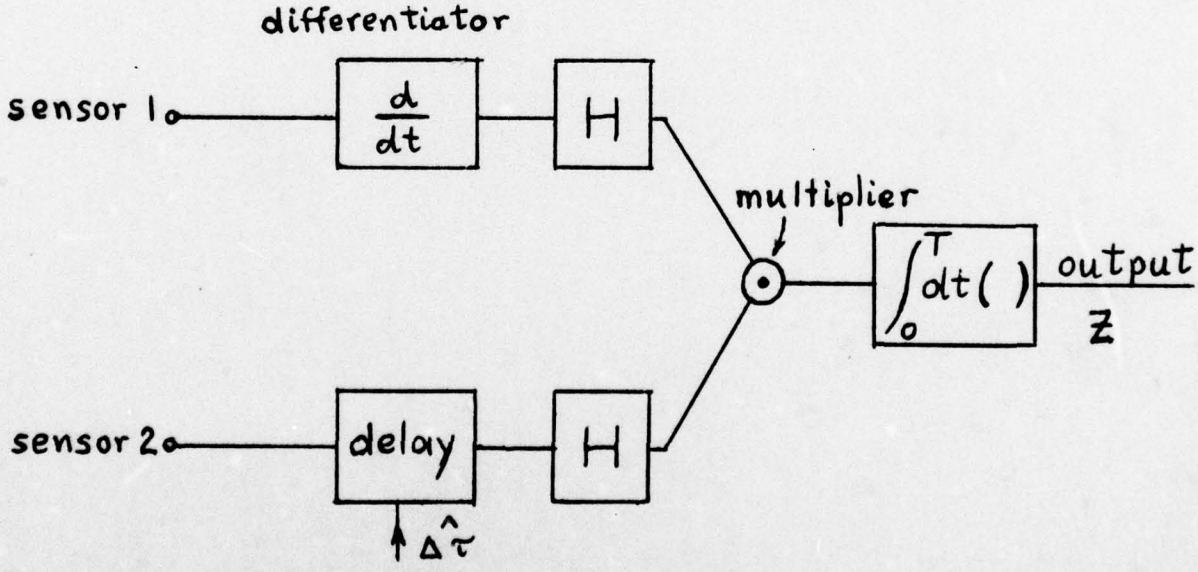

Figure 7

---

[1] A more realistic model would work with directional sensors, but this should have little influence on the ambiguity problem discussed here.

[2] W. J. Bangs, Array Processing with Generalized Beamformers, Report No. 1, Contract N000140-72-C-1293, NUSC Sept. 1971.

When the delay $\hat{\Delta\tau}$ introduced at the output of sensor 2 matches the actual delay $\Delta\tau$ of the signal at sensor 1 relative to that at sensor 2, the expected output E(z) is zero. Thus one need only adjust $\hat{\Delta\tau}$ until the output reaches a null and use its value as an estimate of $\Delta\tau$ and hence of differential delay.

If the signal is a pure sinusoid, E(z), considered as a function of $\hat{\Delta\tau}$, will simply be a sinusoid. It will then have an infinite number of nulls at all values of $\hat{\Delta\tau}$ corresponding to differential delays differing from the true value by a multiple of the signal period. If the signal is a narrowband process one would expect basically similar behavior, with one important difference: The plot of E(z) vs $\hat{\Delta\tau}$ will now have an envelope as suggested in Fig. 8. It will still have a series of nulls,

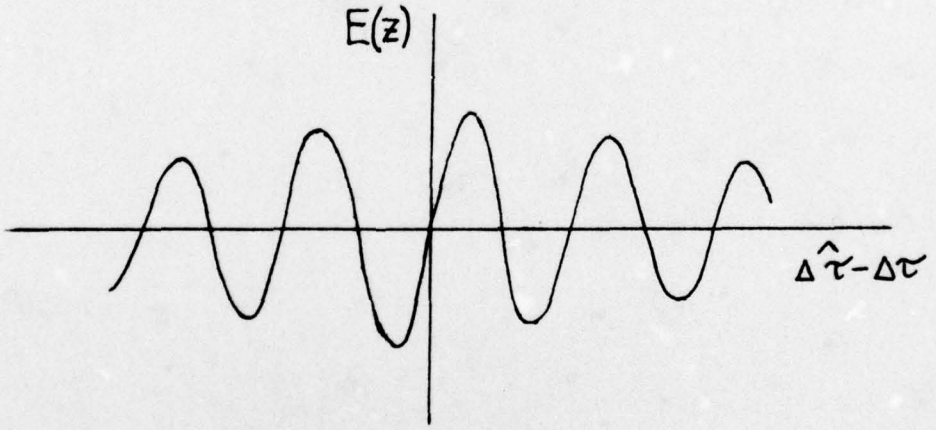

Figure 8

but the fact that the peak closest to the correct null is higher than all others provides a means of resolving the ambiguity.

If the signal bandwidth is very small compared to its center frequency, the envelope of Fig. 8 decays slowly and the difference in height of successive maxima becomes difficult to detect. As a measure of this

difficulty we compute the difference in the values of E(z) at two successive maxima and divide it by the "typical fluctuation noise", the rms value of the fluctuation of z.

An analytical expression for E(z) can be extracted from the previously cited reference[1]. Assuming a signal spectrum of level S flat over the band $\omega_0 - \Delta\omega \leq \omega \leq \omega_0 + \Delta\omega$ we obtain[2]

$$E(z) = \frac{ST}{\pi}\left\{\frac{1}{(\hat{\Delta\tau} - \Delta\tau)^2} \sin \Delta\omega(\hat{\Delta\tau} - \Delta\tau) \cos \omega_0(\hat{\Delta\tau} - \Delta\tau)\right.$$

$$- \frac{1}{\hat{\Delta\tau} - \Delta\tau} [\Delta\omega \cos \omega_0(\hat{\Delta\tau} - \Delta\tau)\cos \Delta\omega(\hat{\Delta\tau} - \Delta\tau)$$

$$\left. - \omega_0 \sin \omega_0(\hat{\Delta\tau} - \Delta\tau) \sin \Delta\omega(\hat{\Delta\tau} - \Delta\tau)]\right\}. \qquad (39)$$

For small $\Delta\omega/\omega_0$ the first two maxima of E(z) (above $\hat{\Delta\tau} = \Delta\tau$) should occur very close to $\pi/(2\omega_0)$ and $5\pi/(2\omega_0)$ respectively. Evaluating E(z) at these two points and using the approximation $\Delta\omega/\omega_0 << 1$ one obtains

$$E(z)\Big|_{\hat{\Delta\tau}-\Delta\tau = \frac{\pi}{2\omega_0}} - E(z)\Big|_{\hat{\Delta\tau}-\Delta\tau = \frac{5\pi}{2\omega_0}} \simeq ST\omega_0{}^2\pi\left(\frac{\Delta\omega}{\omega_0}\right)^3. \qquad (40)$$

The standard deviation of z should not vary greatly over an interval of one, or even several, cycles in Fig. 8. We can therefore work with its value at $\hat{\Delta\tau} = \Delta\tau$.[3] The required analytical formulation is again contained

---

[1] W. J. Bangs, p. 101, p. 157.

[2] The filter H in Fig. 7 is here simply a perfect bandpass filter matched to the signal band.

[3] The exact expression for arbitrary $\hat{\Delta\tau} - \Delta\tau$ is not difficult to obtain, but is quite cumbersome.

in the cited report[1]. To the same order of approximation as in Eq. (40)

$$D(z) \simeq \sqrt{\frac{T\Delta\omega}{2\pi}} \quad N\sqrt{1 + 2\frac{S}{N}}\omega_0 \tag{41}$$

where N is the white noise power level at each receiver.

Hence the figure of merit for our ability to resolve the ambiguity is

$$\frac{E(z)\Big|_{\Delta\hat{\tau} - \Delta\tau = \frac{\pi}{2\omega_0}} - E(z)\Big|_{\Delta\hat{\tau} - \Delta\tau = \frac{5\pi}{2\omega_0}}}{D(z)}$$

$$\simeq \sqrt{2\pi^3 \frac{(\frac{S}{N})^2}{1 + 2\frac{S}{N}}} \quad \sqrt{T\Delta\omega} \quad (\frac{\Delta\omega}{\omega_0})^2 \tag{42}$$

If we are to distinguish the height of successive peaks and hence identify the proper null, we must certainly have a figure of merit well in excess of unity. For a 1% bandwidth and high signal to noise ratio the required condition is

$$T\Delta\omega > \frac{10^8}{\pi^3 \frac{S}{N}} \simeq \frac{3.2 \times 10^6}{S/N} \tag{43}$$

Unless ω_0 (and hence $\Delta\omega$) is large this can easily lead to exceedingly large observation times.[2]

It is, of course, not necessary to resolve adjacent nulls of Fig. 8

---

[1] W. J. Bangs, p. 38.

[2] The strictly linear S/N dependence for large signal to noise ratios results from the use of D(z) at $\Delta\hat{\tau} = \Delta\tau$. A more exact computation would result in a figure of merit which saturates at very high S/N.

in order to gain some benefit from the coherent processing procedure. When the signal frequency is high and differential distances of a wavelength are therefore quite small, considerable gains can be made by identifying the location of the true null within 10 or 20 periods of Fig. 8. The extent to which this is possible clearly depends on the envelope of Fig. 8. What we have considered here is only one possible way of utilizing the envelope information.

6. Narrowband Signals: General Considerations.

For the remainder of this report we shall assume that the signal is a narrowband Gaussian process whose spectrum is centered about some frequency ω_0 large compared with the bandwidth. If the bandwidth is extremely small (smaller than the inverse of the observation time) the signal looks essentially like a fixed amplitude sinusoid throughout the observation interval. The problem is then essentially the same as that treated in the previous sections, the only difference being that the amplitude of the received sinusoid is itself a random variable. If a sinusoid of known amplitude is unsatisfactory (because of ambiguity), a sinusoid of the same frequency but unknown amplitude will certainly be no improvement. It follows that the only bandwidths of practical interest are those which are appreciably larger than the inverse of the observation time.

On the other hand, it is necessary to keep in mind that signals of practical interest may have a bandwidth which is quite small compared with the center frequency ω_0. Unless ω_0 is very large, or the observation time is unrealistically long, the time-bandwidth products will therefore not exceed unity by many orders of magnitude. We shall find that this leads to the breakdown of an analytical assumption which has been made very widely in the study of optimal detectors and estimators.

We now turn to the role of the signal envelope. We have seen that the narrowband estimation problem consists of two distinct components

a) Separation of the global maximum of the likelihood function from other maxima.

b) Estimation of the coordinates of the global maximum.

The argument of Section 5 suggests that errors due to a) will far outweigh those due to b) for typical parameter values. With a few widely separated sensors (subarrays) the ability to separate maxima of the likelihood function is governed by the envelope of the signal correlation. [See Fig. (8).] This envelope, in turn, is generated by the signal envelope. One is therefore led to the conjecture that one can envelope detect the beamformed outputs of each subarray and generate the location estimate from a coherent combination of the envelopes without sacrificing any information of real value. An alternative statement of this point of view is the following: It is hopeless to attempt measurement of differential distances to one wavelength, or even a few wavelengths. The only really relevant information in the signal is therefore contained in its slowly varying envelope. We shall adopt this point of view and assume from here on that each subarray output has been envelope detected before further processing. We have no precise measure of what has been thrown away in doing this, but we suspect strongly that the sacrifice is small.

Under these ground rules, the most general estimator assumes the form shown in Fig. 9. The designer is given the envelopes R_i as inputs and must use them to obtain the best estimates of bearing and range. Since the signal is known to have narrow bandwidth, it is reasonable to assume that prior to envelope detection each beamformer output has been processed by a bandpass filter centered about ω_0 and of a bandwidth at least comparable with that of the signal. Thus the noise as well as the signal at the envelope detector inputs has narrowband properties.

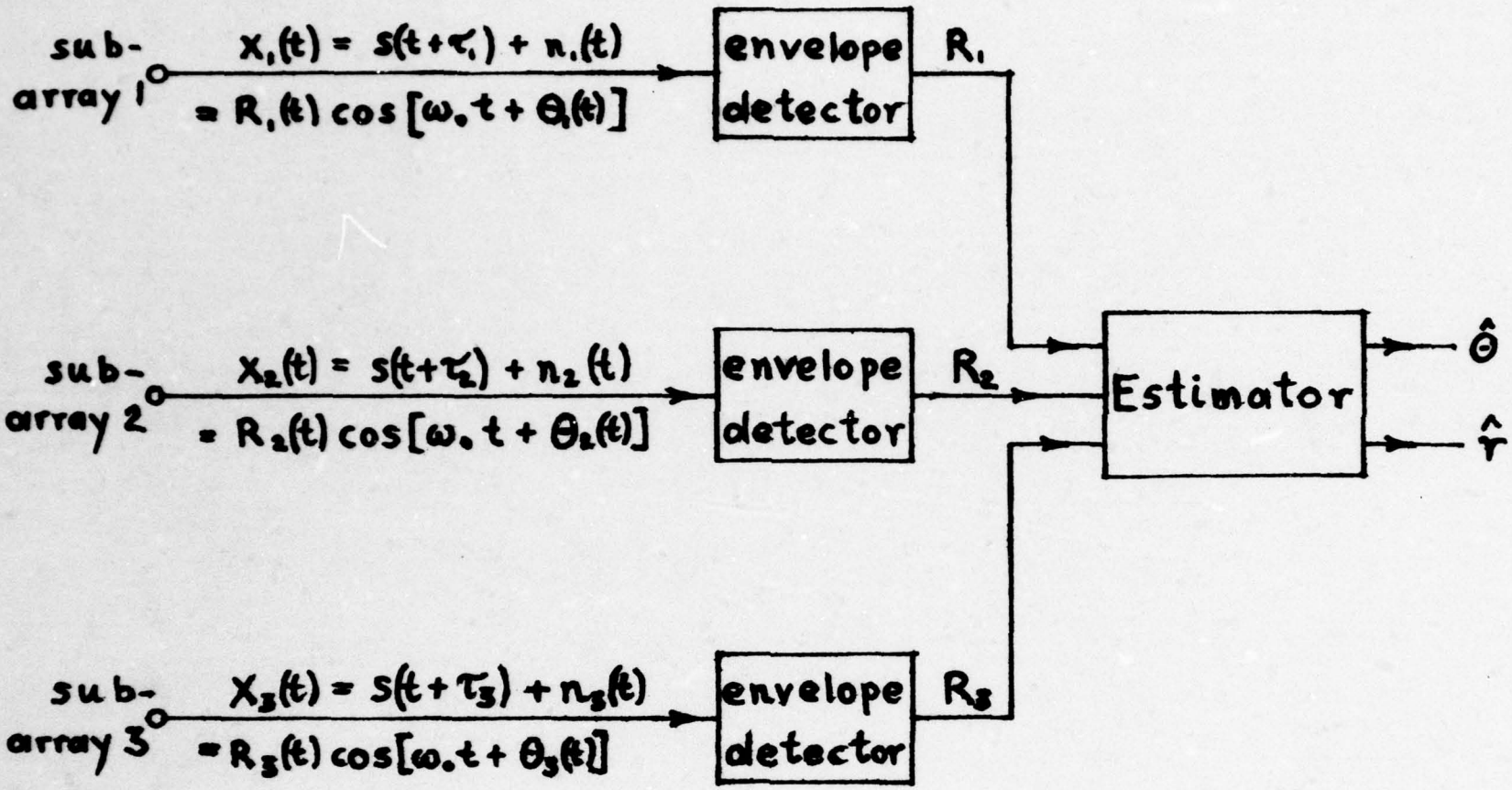
sub-array 1
$X_1(t) = s(t+\tau_1) + n_1(t)$
$= R_1(t)\cos[\omega_0 t + \theta_1(t)]$
envelope detector
R_1
sub-array 2
$X_2(t) = s(t+\tau_2) + n_2(t)$
$= R_2(t)\cos[\omega_0 t + \theta_2(t)]$
envelope detector
R_2
sub-array 3
$X_3(t) = s(t+\tau_3) + n_3(t)$
$= R_3(t)\cos[\omega_0 t + \theta_3(t)]$
envelope detector
R_3
Estimator
$\hat{\theta}$
$\hat{\tau}$

Fig. 9

If signal and noise are independent Gaussian processes the beamformer outputs $x_i(t)$ are Gaussian processes which can be written in envelope and angle form as follows[1]

$$x_i(t) = x_{c_i}(t) \cos \omega_0 t + x_{s_i}(t) \sin \omega_0 t$$

$$= R_i(t) \cos[\omega_0 t + \theta_i(t)] \tag{44}$$

where

$$R_i(t) = \sqrt{x_{c_i}^2(t) + x_{s_i}^2(t)} \tag{45}$$

and

$$\theta_i(t) = \arctan \frac{x_{s_i}(t)}{x_{c_i}(t)} \tag{46}$$

$x_{c_i}(t)$ and $x_{s_i}(t)$ are Gaussian random processes, each with a spectrum obtained from the spectrum of the original narrowband process $x_i(t)$ by downshifting it ω_0 *rad/sec.*

It is apparent from Eq. (45) that $R_i(t)$ is not a Gaussian random process. In fact, it is a simple matter to demonstrate that for any given t the random variable $R_i(t)$ has a Rayleigh distribution. To characterize the estimator input statistically one needs the joint distributions of the $R_i(t_j)$ for many observation instants t_j. It is not difficult to write this distribution down formally, but it is extremely difficult to infer from it the performance of the maximum likelihood estimator or even the Carmèr-Rao bound. Efforts to proceed along these lines were entirely unsuccessful. An alternative approach was therefore taken.

If one assumes that the pre-envelope processes $x_{c_i}(t)$ and $x_{s_i}(t)$, i = 1, 2, 3,

---

[1] See, for instance, S. O. Rice, Mathematical Analysis of Random Noise, B. S. T. J., Jan. 1975.

are separately available at the estimator input (which they are not), the data vector becomes Gaussian and the estimation procedure is well understood. One can immediately write down the relevant estimation errors from results available in the literature. Since the input processes $R_i(t)$ can be constructed from the $x_{c_i}(t)$ and $x_{s_i}(t)$ [by using Eq. (45)], but not vice versa, such calculations yield lower bounds on the errors attainable with the instrumentation of Fig. 9.

Upper bounds on estimation error can be obtained by considering any particular physically realizable instrumentation. If, with careful choice and some luck, one arrives at an instrumentation whose errors are not too far above the lower bounds, then one can claim to have bracketed the estimation errors attainable with Fig. 9 quite accurately. At the same time one has described an instrumentation which comes reasonably close to the optimum. That this is indeed possible, at least over important ranges of the interesting parameters, is demonstrated in a later section.

7. Lower Bound on Estimation Error

Bangs has solved the problem of optimum bearing and range estimation using a set of sensors each of which puts out a Gaussian random process[1]. To adapt this result for our purposed we need only recognize that each sensor in our lower bound approximation produces two Gaussian random processes, $x_{c_i}(t)$ and $x_{s_i}(t)$. We must therefore determine the cross-correlation between these two processes. A straightforward computation yields

$$E\{x_{c_i}(t_1)x_{s_i}(t_2)\} = \int_0^\infty G_i(\omega)\, \sin[(\omega - \omega_0)(t_2 - t_1)]\, d\omega \,. \tag{47}$$

$G_i(\omega)$ is the spectrum of the narrowband process $x_i(t)$ produced by the i^{th} sensor. When $t_2 = t_1$ the integrand of Eq. (47) is zero, confirming the well-known results that the two pre-envelope functions $x_{c_i}(t)$ and $x_{s_i}(t)$ are statistically independent when observed at the same time. A similar claim is not true in general for $t_2 \neq t_1$. However, if the spectrum of the narrowband process is symmetrical about ω_0, i.e.

$$G_i(\omega) = G(\omega - \omega_0) \tag{48}$$

with G(x) an even function, then

$$E\{x_{c_i}(t_1)x_{s_i}(t_2)\} = \int_{-\omega_0}^\infty G(x)\, \sin\left[(t_2 - t_1)\, x\right] dx \;\simeq\; 0 \tag{49}$$

The only approximation implied in Eq. (49) is that the bandwidth of the process is sufficiently small compared with ω_0 so that the lower limit can be replaced with $-\infty$. In that case the $x_{s_i}(t)$ yield a data set completely independent of the $x_{c_i}(t)$. One can then work with either member of the pair and reduce the calculated mean square errors by a factor of two. The results of Bangs[2] analysis are now applicable with only trivial modification.

---

[1] W. J. Bangs, Array Processing with Generalized Beamformers, Report No. 1, Contract N00140-72-C-1293, NUSC, Sept. 1971.

[2] W. J. Bangs, p. 97.

a) Two subarrays

In the simplest case there are only two subarrays. Since we are modelling each of these as an omnidirectional sensor[2] we can only estimate differential delay (i.e. we can only identify the hyperbola on which the source is located). The general expression for the estimation error is

$$D^2(\hat{\tau}) = \{\frac{2T}{\pi} \int_0^{\infty} \frac{\omega^2 [S(\omega)/N(\omega)]^2}{1 + 2S(\omega)/N(\omega)} \, d\omega \}^{-1} \tag{50}$$

$S(\omega)$ and $N(\omega)$ are the signal and noise spectra of the pre-envelopes. Their shape is that of the narrowband spectra downshifted in frequency by ω_0.

If the signal to noise ratio is constant (S/N) over the signal band $0 \leq \omega \leq \Delta\omega$ and zero elsewhere a simple calculation yields

$$D^2(\hat{\tau}) = \frac{3\pi}{2} \frac{1}{(\Delta\omega)^2} \frac{1}{T\Delta\omega} \frac{1 + 2S/N}{(S/N)^2}. \tag{51}$$

In order to gain some intuitive feeling for the magnitude of this error, suppose that the source is remote compared with the subarray spacing, so that error in differential delay can be translated into bearing error.

$$D^2(\hat{\theta}) = \frac{3}{8\pi} \frac{1}{T\Delta\omega} \left(\frac{\lambda_M}{D \sin\theta}\right)^2 \frac{1 + 2S/N}{(S/N)^2} \tag{52}$$

Here λ_M is the wavelength of the highest modulation frequency, related to $\Delta\omega$ by

$$\lambda_M = \frac{2\pi c}{\Delta\omega} \tag{53}$$

As an example, suppose $D = 10^4\lambda$, $\lambda_M = 1000\,\lambda$ (0.1% bandwidth) and S/N = 10. With these numerical values the rms bearing error is

$$D(\hat{\theta}) \tilde{=} \frac{0.9}{\sqrt{T\Delta\omega} \sin\theta} \text{ degrees} \tag{54}$$

Thus, even with this extremely narrowband signal, one does not require excessively large $T\Delta\omega$ products in order to obtain reasonable bearing accuracy.

---

[2] With a signal to noise ratio equal to the post-beamforming signal to noise ratio of the subarray.

b) Three subarrays.

The problem becomes more interesting when there are three subarrays. Consider the geometrical arrangement shown in Fig. 10. Assuming signal to noise ratios constant over the signal band the mean square bearing and range errors can be written down immediately[1]

$$D^2(\hat{\theta}) = \frac{3\pi(1 + 3\frac{S}{N})}{T\Delta\omega(\frac{S}{N})^2} \frac{1}{(\Delta\omega)^2} \frac{1}{Tr(\underline{\tau}_\theta \underline{\tau}_\theta^\dagger)} \frac{1}{1 - \rho_{r\theta}} . \tag{55}$$

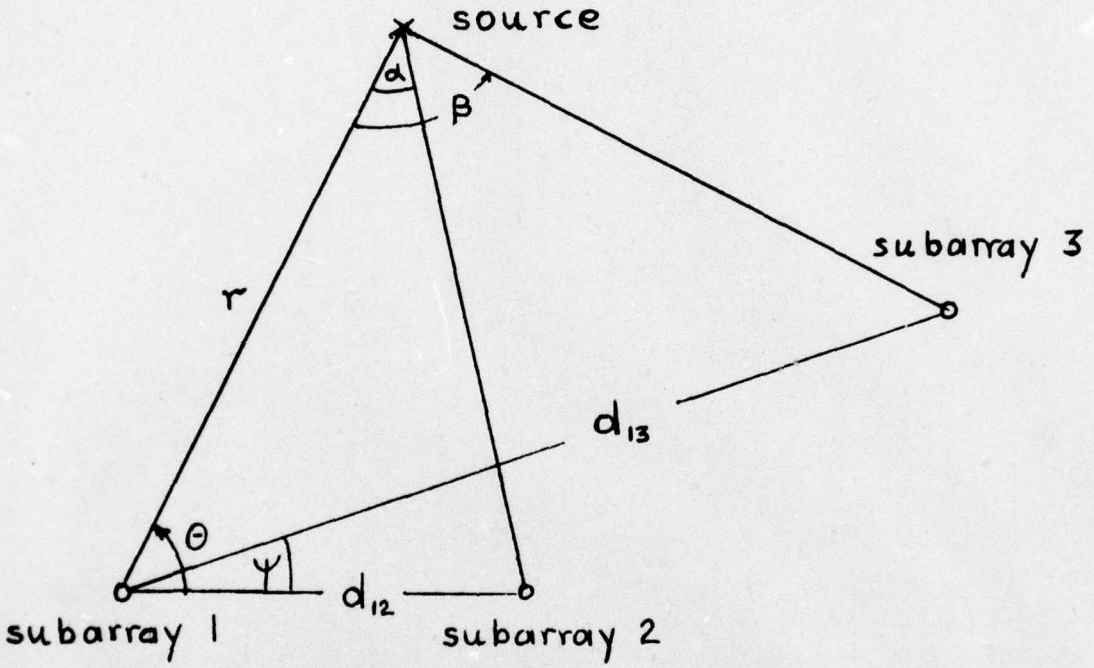

Fig. 10

$$D^2(\hat{r}) = \frac{3\pi(1 + 3\frac{S}{N})}{T\Delta\omega(S/N)^2} \frac{1}{(\Delta\omega)^2} \frac{1}{Tr(\underline{\tau}_r \underline{\tau}_r^\dagger)} \frac{1}{1 - \rho_{r\theta}} . \tag{56}$$

---

[1] W. J. Bangs, p. 106. The superscript † denotes the transpose - conjugate of a matrix.

The matrices $\underline{\tau}_\theta$ and $\underline{\tau}_r$ are composed of purely geometrical factors.

$$[\underline{\tau}_\theta]_{ij} = \frac{\partial \tau_i}{\partial \theta} - \frac{\partial \tau_j}{\partial \theta} \tag{57}$$

$$[\underline{\tau}_r]_{ij} = \frac{\partial \tau_i}{\partial r} - \frac{\partial \tau_j}{\partial r} \tag{58}$$

τ_i is the travel time of the signal from the source to the i^{th} subarray.

The parameter $\rho_{r\theta}$ in Eqs. (55) and (56) describes the dependence between the bearing and range measurements. It is given by the expression

$$\rho_{r\theta} = \frac{[\mathrm{Tr}(\underline{\tau}_r \underline{\tau}_\theta^{\dagger})]^2}{\mathrm{Tr}(\underline{\tau}_\theta \underline{\tau}_\theta^{\dagger})\mathrm{Tr}(\underline{\tau}_r \underline{\tau}_r^{\dagger})} \tag{59}$$

$\rho_{r\theta} = 0$ indicates independence of the measurements,

$\rho_{r\theta} = 1$ implies complete dependence.

The matrix elements given by Eqs. (57) and (58) are easily computed. They assume a very simple form when expressed in terms of the angles α and β subtended at the source by the various array pairs.

$$\frac{\partial \tau_1}{\partial \theta} = 0, \quad \frac{\partial \tau_2}{\partial \theta} = \frac{r}{c} \sin \alpha, \quad \frac{\partial \tau_3}{\partial \theta} = \frac{r}{c} \sin \beta \tag{60}$$

$$\frac{\partial \tau_1}{\partial r} = \frac{1}{c}, \quad \frac{\partial \tau_2}{\partial r} = \frac{1}{c} \cos \alpha, \quad \frac{\partial \tau_3}{\partial r} = \frac{1}{c} \cos \beta. \tag{61}$$

Straightforward computations now yield the geometrical factors required in Eqs. (55) and (56)

$$\mathrm{Tr}(\underline{\tau}_\theta \underline{\tau}_\theta^{\dagger}) = \frac{2r^2}{c^2} \{\sin^2\alpha + \sin^2\beta + (\sin \alpha - \sin \beta)^2\} \tag{62}$$

$$\mathrm{Tr}(\underline{\tau}_r \underline{\tau}_r^{\dagger}) = \frac{2}{c^2} \{(1 - \cos \alpha)^2 + (1 - \cos \beta)^2 + (\cos\alpha - \cos \beta)^2\} \tag{63}$$

$$\rho_{r\Theta} = \frac{\{\sin\alpha(\cos\alpha - 1) + \sin\beta(\cos\beta - 1) + (\sin\beta - \sin\alpha)(\cos\beta - \cos\alpha)\}^2}{[\sin^2\alpha + \sin^2\beta + (\sin\alpha - \sin\beta)^2][(1-\cos\alpha)^2 + (1-\cos\beta)^2 + (\cos\alpha - \cos\beta)^2]} \tag{64}$$

A numerical example is worked out in Fig. 11 for S/N = 10. Note that the angles α and β decrease from the top to the bottom of the table.

α	β	$\rho_{r\Theta}$	$\frac{\hat{D(r)}}{\lambda_M}\sqrt{T\Delta\omega}$	$\frac{r}{\lambda_M} D(\hat{\Theta})\sqrt{T\Delta\omega}$
60°	120°	0.57	0.13	3.1°
45°	90°	0.80	0.28	16°
30°	45°	0.92	1.6	36°
10°	20°	0.92	7.2	75°
5°	10°	0.92	29	151°

Fig. 11

This implies that the source is more and more distant compared to the spacing between subarrays. The correlation coefficient $\rho_{r\Theta}$ increases at first, but then quickly approaches an asymptotic value as the angles α and β decrease. For a remote source the correlation coefficient is quite close to unity, indicating strong coupling between bearing and range measurements.[1] The fourth column of Fig. 11 gives the normalized range error (in units of modulation wavelength). Once the source is remote compared with the interarray spacing (last two entries) the range error increases with the square of the actual range as one would expect. The last column gives the

[1] It is possible to reduce the coupling by choosing the reference point (from which bearing and range are measured) near the center of the overall array rather than at one end.

normalized bearing error. Note that the normalization includes the value of r. For large ranges the actual bearing error becomes independent of r, as one would anticipate.

The analytical expressions of Eqs. (55) and (56) are quite complex. Very much simpler forms result if the actual range happens to be large compared with the interarray spacing (although no assumption to that effect is made in obtaining the estimate).

$$D^2(\hat{\theta}) \simeq \frac{3}{16\pi} \frac{1}{T\Delta\omega} \frac{1 + 3\ S/N}{(S/N)^2} \left(\frac{\lambda_M}{d_{13}}\right)^2 \frac{1}{1 - \rho_{r\theta}} \cdot$$

$$\frac{1}{\sin^2(\theta - \psi) + \left(\frac{d_{12}}{d_{13}}\right)^2 \sin^2\theta - \frac{d_{12}}{d_{13}} \sin\theta \sin(\theta - \psi)} \tag{65}$$

$$D^2(\hat{r}) \simeq \frac{3}{2\pi} \frac{1}{T\Delta\omega} \frac{1 + 3\ S/N}{(S/N)^2} \left(\frac{\lambda_M r^2}{d_{13}^2}\right)^2 \frac{1}{1 - \rho_{r\theta}}$$

$$\frac{1}{\sin^4(\theta - \psi) + \left(\frac{d_{12}}{d_{13}}\right)^4 \sin^4\theta + \left[\sin^2(\theta - \psi) - \left(\frac{d_{12}}{d_{13}}\right)^2 \sin^2\theta\right]^2} \tag{66}$$

Suppose, in particular, that the 3 subarrays are arranged in a straight line ($\psi = 0$) and are equally spaced ($d_{13} = 2\ d_{12}$). Then

$$D^2(\hat{\theta}) \simeq \frac{1}{4\pi} \frac{1}{T\Delta\omega} \frac{1 + 3\ S/N}{(S/N)^2} \left(\frac{\lambda_M}{d_{13} \sin\theta}\right)^2 \frac{1}{1 - \rho_{r\theta}} \tag{67}$$

$$D^2(\hat{r}) \simeq \frac{12}{13\pi} \frac{1}{T\Delta\omega} \frac{1 + 3\ S/N}{(S/N)^2} \left(\frac{\lambda_M r}{d_{13}^2 \sin^2\theta}\right)^2 r^2 \frac{1}{1 - \rho_{r\theta}} \cdot \tag{68}$$

For large actual ranges the correlation coefficient $\rho_{r\theta}$ reduces to

$$\rho_{r\theta} = \frac{\{\sin^3(\theta-\psi)+(\frac{d_{12}}{d_{13}})^3\sin^3\theta - \frac{1}{2}[\sin(\theta-\psi) + \frac{d_{12}}{d_{13}}\sin\theta]\frac{d_{12}}{d_{13}}\sin(\theta-\psi)\sin\theta\}^2}{[\sin^2(\theta-\psi)+(\frac{d_{12}}{d_{13}})^2\sin^2\theta - \frac{d_{12}}{d_{13}}\sin(\theta-\psi)\sin\theta][\sin^4(\theta-\psi)+(\frac{d_{12}}{d_{13}})^4\sin^4\theta - (\frac{d_{12}}{d_{13}})^2\sin^2(\theta-\psi)\sin^2\theta]} \tag{69}$$

This is independent of r and only a function of array geometry. With $\psi = 0$ and $d_{12} = \frac{1}{2} d_{13}$ it assumes the numerical value

$$\rho_{r\theta} = \frac{12}{13}. \tag{70}$$

It may be interesting to compare the bearing estimate obtained by the 3 subarray configuration with that product by the 2 subarray configuration (under a far-field assumption). We therefore consider the same combination of parameter values as in the earlier case [$d_{13} = 10^4\lambda$, $\lambda_M = 1000\lambda$, S/N = 10]. Eq. (67) now yields

$$D(\hat{\theta}) = \frac{3.2}{\sqrt{T\Delta\omega}\sin\theta} \quad \text{degrees} \tag{71}$$

Comparing with Eq. (54) we find that the 3 subarray configuration is poorer by a factor which is almost precisely equal to $(1 - \rho_{r\theta})^{-1/2}$. In Eq. (54) we assumed prior knowledge to the effect that the source was remote compared with the interarray spacing. Eq. (71) makes no such assumption. Bearing and range must therefore be estimated simultaneously with a resultant degradation in each estimate.

Perhaps the most interesting comparison is that between the 3 subarray system using envelope information only and a single subarray system which, because of the close spacing of sensors, can use the full narrowband signal without encountering serious ambiguity problems. The bearing error of the single subarray system is given by

$$D_1^2(\hat{\theta}) = \frac{3}{2\pi}\frac{1}{T\Delta\omega}\frac{1 + S/N}{(S/N)^2}\left(\frac{\lambda}{L\sin\theta}\right)^2 \tag{72}$$

where S/N is still the post-beamforming signal to noise ratio. Dividing (72) by (67) one obtains

$$\frac{D_1^2(\hat{\Theta})}{D^2(\hat{\theta})} = 6\left(\frac{d_{13}}{L}\cdot\frac{\lambda}{\lambda_M}\right)^2 \frac{1+S/N}{1+3\,S/N}\,(1-\rho_{r\Theta}) \tag{73}$$

Depending on various parameter values this quantity can be either larger or smaller than unity. Suppose, in particular, that $d_{13} = 100\ L$, $\lambda_M = 100\lambda$ (1% bandwidth) and $S/N >> 1$. Then

$$\frac{D_1^2(\hat{\Theta})}{D^2(\hat{\Theta})} \simeq 0.15 \tag{74}$$

For this particular combination of parameters the single array is therefore preferable. In this instance the factor $(1-\rho_{r\Theta})$ plays a key role in degrading the performance of the multiple array system. For the single array, with its relatively short length L, it is quite realistic to assume that the source is in the far field. For the combination of subarrays a similar assumption might be quite unrealistic and one is therefore forced into a joint bearing and range estimation problem.

The corresponding computations for range estimation are quite straightforward. For the parameter values $d_{13} = 10\,\lambda_M$, S/N = 10, Eq. (68) reduces to

$$\frac{D(\hat{r})}{r} \simeq \frac{0.1}{\sqrt{T\Delta\omega}}\,\frac{r}{d_{13}\sin\Theta} \tag{75}$$

To obtain a meaningful measurement this quantity must certainly be small compared to unity. Thus $T\Delta\omega$ must satisfy

$$T\Delta\omega >> 0.01\left(\frac{r}{d_{13}\sin\Theta}\right)^2 \tag{76}$$

For ranges not too large compared with d_{13} this inequality is easy to satisfy. Note, however, that $D^2(r)$ as given by Eq.(68) varies with the square of λ_M. The

required observation time therefore varies as $(\Delta\omega)^{-3}$ and can easily become large if the signal bandwidth is small.

For the single array working with a narrowband signal the mean square range error is[1]

$$D_1^2(\hat{r}) = \frac{45}{8\pi}\frac{1}{T\Delta\omega}\left(\frac{r^2\lambda}{L^2\sin^2\Theta}\right)^2\frac{1+S/N}{(S/N)^2}\frac{1}{1-\rho_{12}} \tag{77}$$

Eq. (77) contains the degradation factor $(1-\rho_{12})^{-1}$ because range measurement with the single subarray is possible only if the signal wavefront has significant curvature over the array. When the source is actually remote, so that $\rho_{r\Theta}$ is close to the asymptotic value given in Eq. (70), then ρ_{12} will certainly be close to the same asymptotic value. It follows from Eqs. (77) and (68) that

$$\frac{D_1^2(\hat{r})}{D^2(\hat{r})} \simeq 6.1\ \frac{1+S/N}{1+3\ S/N}\left[\frac{\lambda}{\lambda_M}\left(\frac{d_{13}}{L}\right)^2\right]^2 . \tag{78}$$

Suppose $d_{13} = 100\ L$ and consider the very small bandwidth $\lambda_M = 1000\ \lambda$. Then for $S/N \gg 1$

$$\frac{D_1^2(\hat{r})}{D^2(\hat{r})} \simeq 200 . \tag{79}$$

Thus the multiple array system is clearly preferable, as one might expect. A similar conclusion should hold for most cases in which the subarray spacing is at all large compared with the dimensions of the individual subarrays.

c) Search area considerations.

The rms bearing and range errors just calculated may be somewhat misleading as a measure of the accuracy with which the source can be located. Fig. 12 illustrates the relevant considerations. We have previously obtained the rms

---

[1] W. J. Bangs, p. 104.

bearing and range errors Δr and $\Delta\Theta$ respectively. We therefore know that, with reasonably high probability, the source is located in the curvilinear rectangle of approximate area $4r\Delta\Theta\Delta r$ shown in the diagram. However, if the range and bearing errors are correlated, the high probability region may actually look more like the dotted ellipse and its area might be significantly smaller.

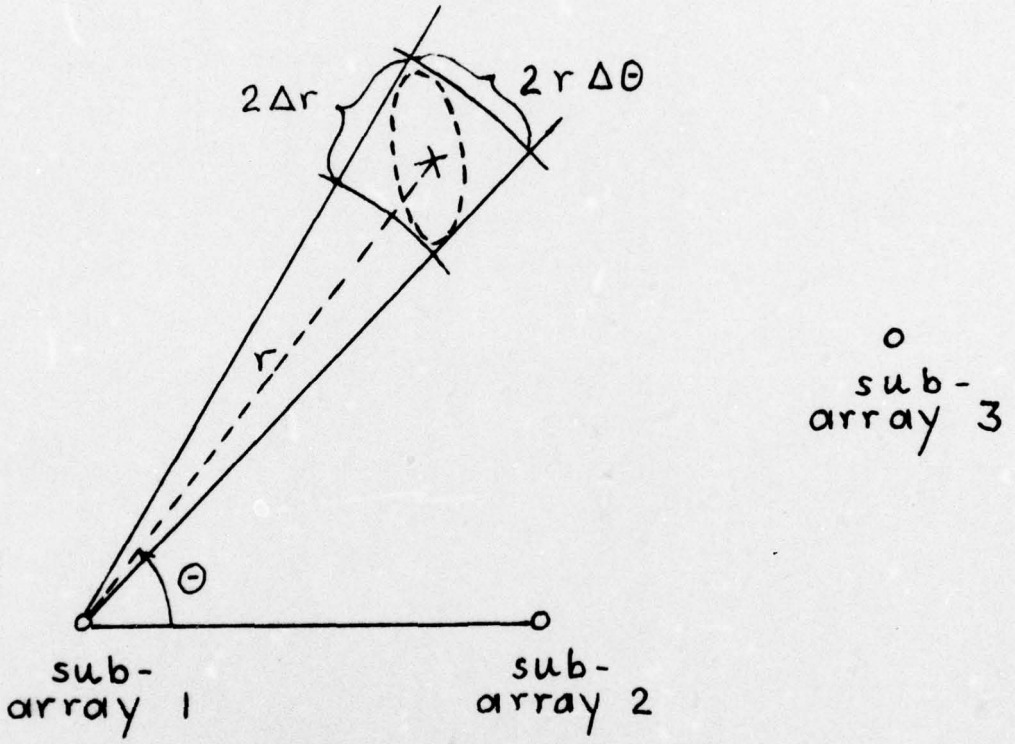

Fig. 12

To gain some insight into this question we use the following generalization of the Cramèr-Rao bound to multidimensional estimation.[1]:

Let $\underline{\varepsilon}$ be the vector of estimation errors and Λ_ε its covariance matrix. Then for any unbiased estimate the concentration ellipse

[1] H. L. Van Trees, Detection, Estimation, and Modulation Theory, Part I, p. 81.

$$\underline{\varepsilon}^T \Lambda_\varepsilon^{-1} \underline{\varepsilon} = C^2 \tag{80}$$

lies outside or on the ellipse

$$\varepsilon^T J \varepsilon = C^2 \tag{81}$$

where J is the Fisher information matrix. As in the one dimensional case, this bound can be approached arbitrarily closely for very long observation times. We therefore calculate the area of the ellipse given by Eq. (81), choosing the constant C somewhat arbitrarily as unity.[1]

For the three subarray configuration the elements of the Fisher information matrix are

$$J_{ij} = \frac{T\Delta\omega}{3\pi} \frac{(S/N)^2}{1 + 3\ S/N} (\Delta\omega)^2\ \mathrm{Tr}(\underline{\tau}_i \underline{\tau}_j^\dagger). \tag{82}$$

The indices i and j can assume the values r and Θ. It is obvious by inspection that our previous results, Eqs. (55) and (56), are simply the elements $[J^{-1}]_{\Theta\Theta}$ and $[J^{-1}]_{rr}$ of the inverse Fisher information matrix.

The uncertainty ellipse described by Eq. (81) with C = 1 has semi-major axis λ_1 and semi-minor axis λ_2, given by the eigenvalues of the covariance matrix $\mathrm{Cov}(r\Delta\Theta, \Delta r)$. Its area is therefore

$$A = \pi\sqrt{\lambda_1\lambda_2} \tag{83}$$

Since the true range r is simply a constant, $\mathrm{Cov}(r\Delta\Theta, \Delta r)$ is very simply related to the Fisher information matrix

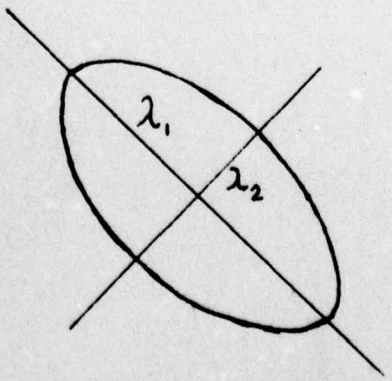

Figure 13

[1] We are thereby defining the region of high probability as that in which the exponent of the (Gaussian) error distribution is no smaller than -1.

$$\mathrm{Cov}(r\Delta\Theta,\ \Delta r) \equiv \begin{bmatrix} \mu_{11} & \mu_{12} \\ \mu_{12} & \mu_{22} \end{bmatrix} = \begin{bmatrix} \frac{J_{\Theta\Theta}}{r^2} & \frac{J_{r\Theta}}{r} \\ \frac{J_{r\Theta}}{r} & J_{rr} \end{bmatrix}^{-1} \tag{84}$$

Eq. (84) defines μ_{11} as the variance of $(r\Delta\Theta)$ and μ_{22} as the variance of Δr.

The eigenvalues of $\mathrm{Cov}(r\Delta\Theta, \Delta r)$ are given by the solutions of the equation

$$\lambda^2 - (\mu_{11} + \mu_{22})\lambda + \mu_{11}\mu_{22} - \mu_{12}^2 = 0. \tag{85}$$

It follows that

$$\lambda_1\lambda_2 = \mu_{11}\mu_{22} - \mu_{12}^2 = \mathrm{Det}[\mathrm{Cov}(r\Delta\Theta,\Delta r)] = \frac{r^2}{\mathrm{Det}\ J}\ . \tag{86}$$

A few lines of algebra now yield the area of the uncertainty ellipse

$$A = \frac{3\pi^2(1 + 3\ S/N)}{\Delta\omega\ T(S/N)^2}\ \frac{r}{(\Delta\omega)^2}\ \frac{1}{\sqrt{\mathrm{Tr}(\underline{\tau}_\Theta\underline{\tau}_\Theta^{\dagger})\mathrm{Tr}(\underline{\tau}_r\underline{\tau}_r^{\dagger})}}\ \frac{1}{\sqrt{1 - \rho_{r\Theta}}}\ .$$

The area of the rectangular uncertainty region in Fig. 12 is given by

$$A_r = 4r\Delta\Theta\Delta r = \frac{12\pi(1 + 3\ S/N)}{\Delta\omega T(S/N)^2}\ \frac{r}{(\Delta\omega)^2}\ \frac{1}{\sqrt{\mathrm{Tr}(\underline{\tau}_\Theta\underline{\theta}_\Theta^{\dagger})\mathrm{Tr}(\underline{\tau}_r\underline{\tau}_r^{\dagger})}}\ \frac{1}{1 - \rho_{r\Theta}}\ . \tag{87}$$

Hence the ratio of the two uncertainty areas is

$$\frac{A_r}{A} = \frac{4}{\pi}\ \frac{1}{\sqrt{1 - \rho_{r\Theta}}}\ . \tag{88}$$

The factor $4/\pi$ is close to unity and is, in any case, somewhat arbitrary, since it depends on the choice of the constant C in Eq. (81). The significant conclusion is that proper exploitation of the dependence between bearing and range estimation can reduce the effective search area by a factor proportional to $(1 - \rho_{r\Theta})^{-1/2}$.

8. Upper bound on estimation error. An envelope tracker.

In the previous section we set lower bounds on the estimation errors attainable with any envelope tracker. To do this we assumed that the pre-envelope functions were available as separate inputs to an optimal estimator. In actual fact the pre-envelope functions are not available to the observer and as a result there is no reason to expect that the calculated error levels are really attainable. In the present section we compute the estimation errors of a particular envelope tracker. No claim is made concerning the optimality of this instrumentation, but since it is clearly realizable, the calculated errors will set upper limits on the minimum estimation errors attainable with any realizable instrumentation.

To keep algebraic complexity within reasonable bounds we consider a configuration using only two subarrays and deal with the estimation of differential delay. Even in a multiple-array system all of the relevant information is contained in the differential delay between the signals received by various subarray pairs. As far as the comparison between the upper and lower bounds is concerned, one therefore feels that the solution for two subarrays should be quite representative of the more general problem.

The system to be analyzed is shown in Fig. 14. It is, in effect, an ordinary two element split beam tracker working with the square of the envelope. The desired estimate of differential delay is the delay $\hat{\tau}$ required in the lower channel to cause the output z to be zero. For Gaussian signals (and large TW products) this instrumentation is known to be optimal. Its operating principle is, in essence, to cross correlate the two channels and determine the delay for which the cross-correlation is a maximum. Since the correlation properties of a random process are not changed drastically by a square law operation, one has some hope that this procedure may still be near-optimal for the non-Gaussian case at hand. The use of the squared envelope, rather than the envelope itself,

as the effective system input it simply a matter of mathematical convenience. R^2 can certainly be constructed from the data as readily as R and the computation therefore yields a legitimate upper bound on the minimum attainable error.

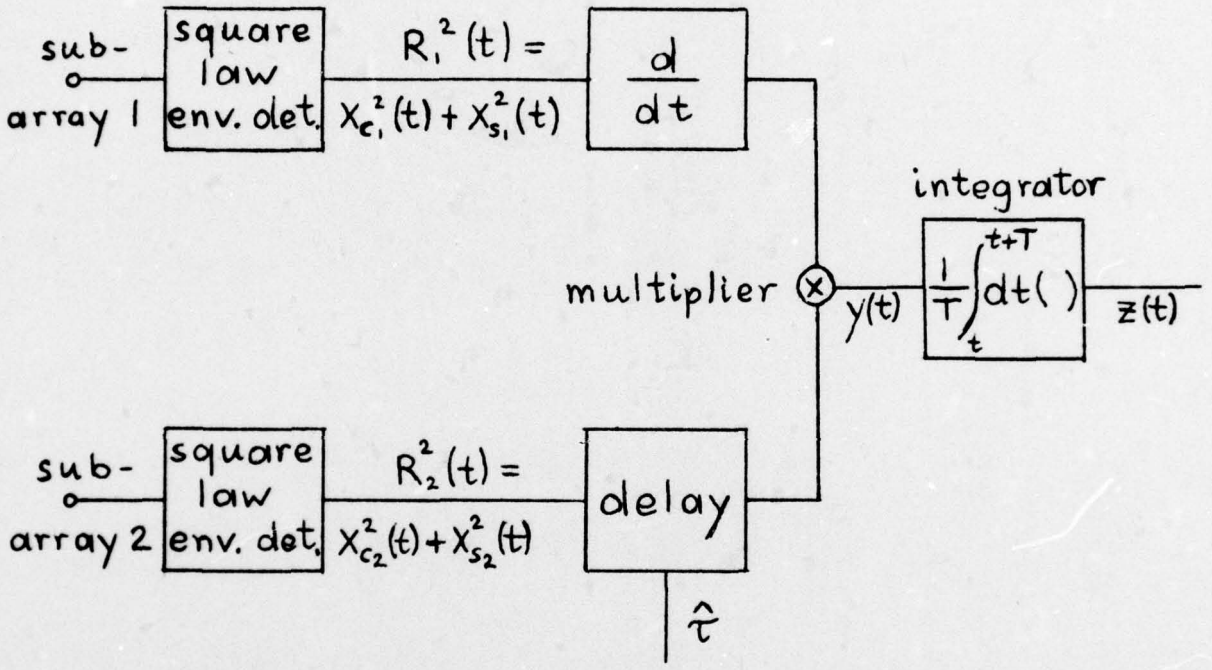

Fig. 14

If the smoothing time T of the integrator is significantly larger than the envelope correlation time, z(t) is approximately Gaussian. The estimator is then unbiased and its mean square error is approximated by[1]

$$D^2(\hat{\tau}) = \frac{D^2(z)\Big|_{\hat{\tau}=\tau}}{\left[\frac{d\bar{z}}{d\hat{\tau}}\Big|_{\hat{\tau}=\tau}\right]^2} \tag{89}$$

τ is the true value of differential delay and $\bar{z}$ is the expected value of z.

[1] W. J. Bangs, §4.3. Eq. (89) assumes that gross ambiguities have been resolved. When only envelope information is used, this should not present a problem.

The denominator of Eq. (89) is easily evaluated

$$\bar{z} = \bar{y} = E\{\frac{d}{dt}[x_{c_1}^2(t) + x_{s_1}^2(t)][x_{c_2}^2(t - \hat{\tau}) + x_{s_2}^2(t - \hat{\tau})]\} \tag{90}$$

Hence

$$\left.\frac{\bar{dz}}{d\tau}\right|_{\hat{\tau} = \tau} = -4E\{[x_{c_1}(t)\dot{x}_{c_1}(t)+x_{s_1}(t)\dot{x}_{s_1}(t)][x_{c_2}(t-\tau)\dot{x}_{c_2}(t-\tau)+x_{s_2}(t-\tau)\dot{x}_{s_2}(t-\tau)]\} \tag{91}$$

$\dot{x}(t)$ stands for the time derivative of $x(t)$.

All of the pre-envelope functions in Eq. (91) are Gaussian random processes. The required fourth order moments are therefore readily calculated. The result is particularly simple because a zero mean Gaussian process and its derivative are uncorrelated, i.e.

$$E\{x(t)\dot{x}(t)\} = 0 \tag{92}$$

For narrowband processes with spectra symmetrical about the center frequency, we concluded in section 7 that the pre-envelopes $x_c(t)$ and $x_s(t - \tau)$ are uncorrelated, regardless of the delay τ. Finally, if the noise is spatially incoherent, the noise components contribute nothing to the average. The delay $\hat{\tau} = \tau$ aligns the signal components in the two channels and one is left with

$$\left.\frac{\bar{dz}}{d\hat{\tau}}\right|_{\hat{\tau}=\tau} = -8\,\overline{x_{c_1}^2(t)} \cdot \overline{\dot{x}_{c_1}^2(t)}\Big|_{\text{noise}=0} . \tag{93}$$

If the signal pre-envelope has autocorrelation $R_s(\tau)$, this reduces to

$$\left.\frac{\bar{dz}}{d\hat{\tau}}\right|_{\hat{\tau}=\tau} = 8\,R_s(0)\,R_s''(0) \tag{94}$$

where $R_s''(0)$ is the second derivative of the signal autocorrelation evaluated at the origin.

The numerator of Eq. (89) is a good deal more tedious to compute. The procedure is straightforward in principle. The variance of z is simply the integral of its spectrum $G_z(\omega)$.

$$D^2(z) = \int_0^\infty G_z(\omega)\, d\omega \tag{95}$$

The spectrum of z is readily obtained from the spectrum of y [see Fig. 14].

$$G_z(\omega) = G_y(\omega)\ |H(\omega)|^2 \tag{96}$$

where $H(\omega)$ is the transfer function of the integrator. $G_y(\omega)$, in turn, is computed from the Fourier transform of the autocorrelation $R_y(\alpha)$.

$$G_y(\omega) = \frac{1}{\pi} \int_{-\infty}^{\infty} R_y(\alpha) e^{-j\omega\alpha}\, d\alpha\ . \tag{97}$$

The computational problem therefore revolves about the determination of $R_y(\alpha)$

$$R_y(\alpha) = E\{y(t)\ y(t+\alpha)\}$$

$$= 4E\{[x_{c_1}(t)\dot{x}_{c_1}(t) + x_{s_1}(t)\dot{x}_{s_1}(t)][x_{c_2}{}^2(t-\hat{\tau}) + x_{s_2}{}^2(t-\hat{\tau})]$$

$$\cdot\ [x_{c_1}(t+\alpha)\dot{x}_{c_1}(t+\alpha) + x_{s_1}(t+\alpha)\dot{x}_{s_1}(t+\alpha)][x_{c_2}{}^2(t-\hat{\tau}+\alpha) + x_{s_2}{}^2(t-\hat{\tau}+\alpha)]\} \tag{98}$$

Multiplying out the four binomials one obtains a number of terms each of which is an 8^{th} order moment of jointly Gaussian random variables. Each such 8^{th} order moment consists of all possible combinations of second order moments taken four at a time, of which there is a very large number. Many of the terms are identical and the computational problem is almost entirely one of keeping an accurate count of terms of various types. Fortunately there is a systematic scheme for doing this[1]. The algebraic details are extremely

[1] J. H. Laning and R. H. Battin, Random Processes in Automatic Control, McGraw-Hill, 1956, p. 82-85.

tedious and without interest in this discussion. We therefore only state the final result

$$R_y(\alpha) = 8\{[-R_s(\alpha)R_s''(\alpha)-(R_s'(\alpha))^2][16R_s^2(0)+4R_N^2(0)+16R_s(0)R_N(0) + 8R_s^2(\alpha) + 8R_N^2(\alpha) + 8R_s(\alpha)R_N(\alpha)]$$

$$+ [-R_N(\alpha)R_s''(\alpha) - R_N'(\alpha)R_s'(\alpha)][8R_s^2(0) + 4R_N^2(0) + 8R_s(0)R_N(0) + 8R_s^2(\alpha) + 4R_N^2(\alpha) + 4R_N(\alpha)R_s(\alpha)]$$

$$+ [-R_s(\alpha)R_N''(\alpha) - R_s'(\alpha)R_N'(\alpha)][8R_s^2(0) + 4R_N^2(0) + 16\,R_s(0)R_N(0) + 8R_s^2(\alpha) + 4R_N^2(\alpha) + 12R_N(\alpha)R_s(\alpha)]$$

$$+ [-R_N(\alpha)R_N''(\alpha) - (R_N'(\alpha))^2][4R_s^2(0) + 4R_N^2(0) + 8R_N(0)R_s(0) + 4R_s^2(\alpha) + 4R_N^2(\alpha) + 8R_s(\alpha)R_N(\alpha)]$$

$$+ 16(R_s'(\alpha))^2[R_s^2(\alpha) + R_s(\alpha)R_N(\alpha)] - 8R_s'(\alpha)R_N'(\alpha)R_s(\alpha)R_N(\alpha) - 8R_s(\alpha)R_N''(\alpha)R_s^2(0) - 4R_N(\alpha)R_N''(\alpha)R_s^2(0)\}. \quad (99)$$

$R_N(\alpha)$ is the autocorrelation of the noise pre-envelope.

To proceed further we must assume a particular form of the signal and noise pre-envelope autocorrelations. For computational convenience we choose

$$R_s(\alpha) = Pe^{-\frac{\sigma^2\alpha^2}{2}} \quad (100)$$

$$R_N(\alpha) = Ne^{-\frac{k\sigma^2\alpha^2}{2}} \quad (101)$$

P is the total signal power and N the total noise power. k is a numerical constant which governs the relation between the signal and noise bandwidths. In practice the noise bandwidth would be determined primarily by the bandwidth

of the processing system (since the received noise is likely to have a spectrum flat over a band much larger than that occupied by the signal). The processing band could at best be matched to the signal, leading to a value k = 2 (because the processing filter also affects the signal). If the center frequency of the narrowband signal is not known precisely, one might use a substantially larger processing bandwidth and hence a larger value k.

Substituting Eqs. (100) and (101) into Eq. (99) and evaluating the Fourier integral of Eq. (97) one obtains

$$
\begin{aligned}
G_y(\omega) = \frac{8\sigma}{\sqrt{\pi}} \{ & P^4 \frac{\omega^2}{\sigma^2}\left(8e^{-\frac{\omega^2}{4\sigma^2}} + \sqrt{2}\, e^{-\frac{\omega^2}{8\sigma^2}}\right) \\
& + P^3N\Big[8\frac{\omega^2}{\sigma^2} e^{-\frac{\omega^2}{4\sigma^2}} + \frac{8\sqrt{2}}{\sqrt{k+1}}\left(\frac{k}{k+1} + \frac{1+2k+2k^2}{(k+1)^2}\frac{\omega^2}{\sigma^2}\right) e^{-\frac{\omega^2}{2(k+1)\sigma^2}} \\
& \quad + \frac{8\sqrt{2}}{\sqrt{k+3}}\left(\frac{3k+1}{k+3} + \frac{5+2k+k^2}{(k+3)^2}\frac{\omega^2}{\sigma^2}\right) e^{-\frac{\omega^2}{2(k+3)\sigma^2}}\Big] \\
& + P^2N^2\Big[2\frac{\omega^2}{\sigma^2} e^{-\frac{\omega^2}{4\sigma^2}} + \frac{8\sqrt{2}}{\sqrt{k+1}}\frac{2k+1}{k+1}\frac{\omega^2}{\sigma^2} e^{-\frac{\omega^2}{2(k+1)\sigma^2}} \\
& \quad + \left(2\sqrt{k} + \frac{3}{\sqrt{k}}\frac{\omega^2}{\sigma^2}\right) e^{-\frac{\omega^2}{4k\sigma^2}} \\
& \quad + \frac{2}{\sqrt{k+1}}\left(\frac{k^2+8k+3}{k+1} + \frac{5k^2+6k+5}{2(k+1)^2}\frac{\omega^2}{\sigma^2}\right) e^{-\frac{\omega^2}{4(k+1)\sigma^2}}\Big] \\
& + PN^3\Big[\frac{4\sqrt{2}}{\sqrt{k+1}}\frac{\omega^2}{\sigma^2} e^{-\frac{\omega^2}{2(k+1)\sigma^2}} + \frac{8}{2\sqrt{k}}\frac{\omega^2}{\sigma^2} e^{-\frac{\omega^2}{4k\sigma^2}} \\
& \quad + \frac{4\sqrt{2}}{\sqrt{3k+1}}\left(4k\frac{k+1}{3k+1} + \frac{1+2k+5k^2}{(3k+1)^2}\frac{\omega^2}{\sigma^2}\right) e^{-\frac{\omega^2}{2(3k+1)\sigma^2}}\Big] \\
& + N^4\Big[2\sqrt{k}\frac{\omega^2}{\sigma^2} e^{-\frac{\omega^2}{4k\sigma^2}} + \left(\sqrt{2k} + \frac{1}{2\sqrt{2k}}\frac{\omega^2}{\sigma^2}\right) e^{-\frac{\omega^2}{8k\sigma^2}}\Big]\Big\}
\end{aligned}
\tag{102}
$$

Eq. (102) is still very cumbersome. It is reproduced in full primarily in order to make the following observation. The equation has two types of terms: Those which contain a factor (ω^2/σ^2) and those which do not. There are 14 of the former and only 6 of the latter. σ is the bandwidth of the signal. If $T\sigma >> 1$ (large TW product) the bandwidth of the T second integrator in Fig. 14 is small compared with σ, so that the terms containing the factor (ω^2/σ^2) contribute little to the output variance compared with terms which have no such factor. Before discarding the (ω^2/σ^2) terms, however, it is important to note that there are no terms in P^4 which do not contain (ω^2/σ^2). To discard all terms containing (ω^2/σ^2) would lead to the obviously false result that the output variance is zero in the absence of noise. More specifically, we shall find that the terms not containing (ω^2/σ^2) yield contributions to the output variance of order $(T\sigma)^{-1}$, while those containing (ω^2/σ^2) yield contributions of order $(T\sigma)^{-2}$. For large $(T\sigma)$ products and moderate signal to noise ratios the former are clearly dominant. For large signal to noise ratios and only moderate $(T\sigma)$ products the latter may assume primary importance.

There remains the identification of the integrator transfer function $H(\omega)$ and the evaluation of the output variance from Eq. (95). The transfer function of a T second integrator is

$$H(\omega) = \frac{1}{T}\,\frac{1 - e^{-j\omega T}}{j\omega} \,. \tag{103}$$

The quantity $|H(\omega)|^2$ required in Eq. (96) is therefore

$$|H(\omega)|^2 = \frac{\sin^2 \frac{\omega T}{2}}{(\frac{\omega T}{2})^2} \,. \tag{104}$$

The remainder of the computational procedure is straightforward and we

pass immediately to the final result for estimation error.

$$D^2(\hat{\tau}) = \frac{1}{\sigma^2}\frac{1}{T\sigma}\{\frac{5}{2}\frac{1}{T\sigma}$$

$$+ \frac{N}{P}[\sqrt{2\pi}(\frac{k}{(k+1)^{3/2}} + \frac{3k+1}{(k+3)^{3/2}}) + \frac{2}{T\sigma}(\frac{1+k+2k^2}{(k+1)^2} + \frac{4-k+k^2}{(k+3)^2})]$$

$$+ (\frac{N}{P})^2[\sqrt{\pi}(\sqrt{k} + \frac{1+8k+3k^2}{(k+1)^{3/2}}) + \frac{1}{2T\sigma}(2 + \frac{2+9k}{k+1})]$$

$$+ (\frac{N}{P})^3[\sqrt{2\pi}\frac{2k(k+1)}{(3k+1)^{3/2}} + \frac{1}{T\sigma}(2 + \frac{(k-1)^2}{(3k+1)^2})]$$

$$+ (\frac{N}{P})^4[\frac{\sqrt{2\pi}}{8}\sqrt{k} + \frac{1}{2}\frac{1}{T\sigma}]\}. \qquad (105)$$

When $T\sigma >> 1$ the second term in each power of N/P would tend to be small compared with the first. As anticipated, however, the $(N/P)^0$ contribution only has a term of order $(T\sigma)^{-2}$. For very large signal to noise ratios the magnitude of the $T\sigma$ product therefore becomes critical.

To interpret the k dependence of Eq. (105) properly, it is necessary to keep in mind that N is the total noise power. If the underlying noise is white and its effective bandwidth is determined by the processor bandwidth, then N is proportional to $\sqrt{k}$. In that case the N/P term is asymptotically independent of k, all other noise dependent terms grow with k.

9. Comparison of upper and lower bounds

The primary purpose of analyzing the split beam envelope tracker for the simple configuration of two subarrays was to check whether it could estimate relative delay with anything like optimal efficiency. We must therefore compare Eq. (105) with the comparable result in section 7a. Unfortunately the results in the two sections are not directly comparable as they stand.

In order to keep down computational complexity we used the correlation functions given by Eqs. (100) and (101) [corresponding to Gaussian spectra] in section 8. In order to avoid other computational difficulties in section 7a we worked with signal and noise spectra flat (or at least of identical shape) over the signal band. The result in section 7a [Eq. (51)] therefore involves the signal bandwidth parameter $\Delta\omega$ which is not simply related to the equivalent parameter σ in Eq. (105). To make the upper and lower bounds comparable we return to section 7a, use the spectra introduced in section 8 and circumvent the computational difficulty by finding a lower bound on the resulting integral. We are therefore obtaining a lower bound on the lower bound which, together with Eq. (105), still successfully brackets the attainable minimum mean square error.

The spectra corresponding to Eqs. (100) and (101) are

$$S(\omega) = \sqrt{\frac{2}{\pi}}\,\frac{P}{\sigma}\, e^{-\frac{\omega^2}{2\sigma^2}} \tag{106}$$

$$N(\omega) = \sqrt{\frac{2}{\pi}}\,\frac{N}{\sqrt{k}\,\sigma}\, e^{-\frac{\omega^2}{2k\sigma^2}} \tag{107}$$

Substituting these spectra into Eq. (50) we obtain

$$[D^2(\hat{\tau})]^{-1} = \frac{2T}{\pi} \int_0^{\infty} \frac{\omega^2 \, k \frac{P^2}{N^2} \, e^{-\frac{k-1}{k}\frac{\omega^2}{\sigma^2}}}{1 + 2\sqrt{k}\frac{P}{N} e^{-\frac{k-1}{k}\frac{\omega^2}{2\sigma^2}}}$$

$$\leq \frac{T}{\pi}\sqrt{k}\frac{P}{N} \int_0^{\omega_1} \omega^2 e^{-\frac{k-1}{k}\frac{\omega^2}{2\sigma^2}} d\omega + \frac{2T}{\pi} k \frac{P^2}{N^2} \int_{\omega_1}^{\infty} \omega^2 e^{-\frac{k-1}{k}\frac{\omega^2}{\sigma^2}} d\omega \qquad (108)$$

The upper bound is generated by omitting the first denominator term for $0 \leq \omega \leq \omega_1$ and the second denominator term for $\omega > \omega_1$. The frequency ω_1 will be chosen so that it minimizes the right side of Eq. (108), thus setting the tightest possible bound. The last version of Eq. (108) is readily integrated

$$[D^2(\hat{\tau})]^{-1} \leq \frac{T}{\sqrt{2\pi}}\frac{P}{N}\sqrt{k}\left(\frac{k}{k-1}\right)^{3/2}\sigma^3 \operatorname{erf}\left(\sqrt{\frac{k-1}{k}\frac{\omega_1^2}{2\sigma^2}}\right)$$

$$+ \frac{T}{2\sqrt{\pi}}\left(\frac{P}{N}\right)^2 k \left(\frac{k}{k-1}\right)^{3/2}\sigma^3\left[1 - \operatorname{erf}\sqrt{\frac{k-1}{k}\frac{\omega_1^2}{\sigma^2}}\right]$$

$$+ \frac{T}{\pi}\sigma^2\omega_1 \frac{k}{k-1}\left[k\frac{P^2}{N^2} e^{-\frac{k-1}{k}\frac{\omega_1^2}{\sigma^2}} - \sqrt{k}\frac{P}{N} e^{-\frac{k-1}{k}\frac{\omega_1^2}{2\sigma^2}}\right]. \qquad (109)$$

The error function erf(x) is defined by

$$\operatorname{erf}(x) = \frac{2}{\sqrt{\pi}} \int_0^x e^{-y^2} dy \, . \qquad (110)$$

To find the best value of ω_1 we differentiate the last version of Eq. (108) and set the derivative equal to zero

$$\frac{T}{\pi}\sqrt{k}\frac{P}{N}\omega_1^2 e^{-\frac{k-1}{k}\frac{\omega_1^2}{2\sigma^2}} - \frac{2T}{\pi} k \frac{P^2}{N^2}\omega_1^2 e^{-\frac{k-1}{k}\frac{\omega_1^2}{\sigma^2}} = 0. \qquad (111)$$

A few steps of algebra yield

$$\omega_1 = \sigma \sqrt{\frac{k}{k-1} \ln\left(4k \frac{P^2}{N^2}\right)} \quad . \tag{112}$$

Not surprisingly, Eq. (112) simply gives the value of ω at which the second denominator term in the exact version of Eq. (108) becomes equal to unity. If $4k\, P^2/N^2 < 1$, Eq. (112) is meaningless and one uses $\omega_1 = 0$. Again, this is not surprising, because the signal to noise ratio (after combination of the subarray outputs) is now everywhere smaller than unity.

Substituting Eq. (112) into Eq. (109) one obtains after some algebraic simplification

$$[D^2(\hat{\tau})]^{-1} \leq \frac{T\sigma}{\sqrt{2\pi}} \sigma^2 \left(\frac{k}{k-1}\right)^{3/2} \{\sqrt{k} \frac{P}{N} \operatorname{erf}[\ln(2\sqrt{k} \frac{P}{N})]^{1/2}$$

$$+ \frac{1}{\sqrt{2}} k \frac{P^2}{N^2} [1 - \operatorname{erf}(\ln 4k \frac{P^2}{N^2})^{1/2}]$$

$$- \frac{1}{2\sqrt{\pi}} \sqrt{\ln(2\sqrt{k} \frac{P}{N})} \} \quad . \tag{113}$$

In practice the noise bandwidth is almost certain to be larger than the signal bandwidth ($k > 1$). In that case the error functions very rapidly approach unity as the signal to noise ratio P/N becomes larger than one. Eq. (113) is then dominated by the first term and one can write to an excellent approximation

$$D^2(\hat{\tau}) \geq \frac{\sqrt{2\pi}}{\sigma^2} \frac{1}{T\sigma} \frac{N}{P} \frac{(k-1)^{3/2}}{k^2} \tag{114}^1$$

For very large $T\sigma$ and high signal to noise ratio the split beam tracker error [Eq. (105)] can be approximated by

---

[1] This expression properly goes to zero for $k = 1$, because the signal to noise ratio is then constant at all frequencies.

$$D^2(\hat{\tau})\Big|_{\text{split beam}} \simeq \frac{\sqrt{2\pi}}{\sigma^2}\frac{1}{T\sigma}\frac{N}{P}\left[\frac{k}{(k+1)^{3/2}} + \frac{3k+1}{(k+3)^{3/2}}\right] . \qquad (115)$$

Eqs. (114) and (115) differ only in the k dependent term. In this limit of large $T\sigma$ and high signal to noise ratio one can therefore write the ratio of the upper bound to the lower bound as

$$\frac{\text{Upper bound}}{\text{Lower bound}} = \frac{k^2}{(k-1)^{3/2}}\left[\frac{k}{(k+1)^{3/2}} + \frac{3k+1}{(k+3)^{3/2}}\right] . \qquad (116)$$

Over the practically significant range of k ($k \geq 2$) Eq. (116) is surprisingly insensitive to k. It assumes a value of approximately 4 at $k = 2$, declines to a minimum of about 3.25 near $k = 5$ and then rises to an asymptotic value of 4 as $k \to \infty$. Thus the lower bound falls 5 to 6 db below the upper bound, essentially independent of k.

To interpret this result properly one must keep in mind that the lower bound of Eq. (50) is almost certainly unattainable because it assumes the separate availability of the pre-envelope functions. Furthermore, Eq. (113) only computes a lower bound on this lower bound. It would therefore not be surprising to find Eq. (113) low by as much as 3 db. If this is the case, there is at least a range of $T\sigma$ and P/N for which the simple split beam envelope tracker comes within 3 db of the absolute optimum. One must further keep in mind that no effort has been made to compensate the tracker in Fig. 14 for signal and noise spectral properties. A filter of the Eckart type in each channel would very probably improve its performance relative to the lower bound, quite possibly leaving a differential too small to be of practical concern.

The discrepancy between the upper and lower bound becomes much more pronounced when either of the assumptions $T\sigma \ggg 1$ and $P/N \gg 1$ fails. Consider first the case of small signal to noise ratio.

For P/N << 1, Eq. (105) is dominated by the terms in $(N/P)^3$ and $(N/P)^4$ which are not present in the lower bound at all. The square law envelope detector and multiplier together generate noise intermodulation products of order as high as 4. When P/N << 1 these contribute most of the output fluctuation of the split beam envelope tracker. For low signal to noise ratios one therefore has strong reasons to suspect that the simple instrumentation of Fig. 14 falls well short of the optimum. In practice, of course, no tracker will perform well unless P/N (the post-beamforming signal to noise ratio at each subarray) is reasonably large. This particular shortcoming may therefore be a somewhat academic matter.

A performance limitation of at least potential practical impact results from the tracker's behavior at moderate $T\sigma$ products. If the signal bandwidth is very small it may not be possible to choose T so large that $T\sigma$ exceeds unity by many orders of magnitude. In such a situation the first (noise independent) term of Eq. (105) may make the greatest contribution to the estimation error. Once this happens, further increases in signal to noise ratio will no longer have much effect on the error, which is now determined primarily by signal fluctuations. A plot of mean square error versus P/N will therefore approach a minimum given by

$$D^2(\hat{\tau})\Big|_{min} = \frac{5}{2}\frac{1}{\sigma^2}\frac{1}{(T\sigma)^2} \tag{117}$$

The lower bound of Eq. (113), by contrast, approaches zero as $P/N \to \infty$.

The signal to noise ratio at which Eq. (105) approaches Eq. (117) depends on the relative magnitude of the coefficients of $(N/P)^1$ and $(N/P)^0$. For k in the range $2 \leq k \leq 10$ one finds

$$\sqrt{2\pi}\left[\frac{k}{(k+1)^{3/2}}+\frac{3k+1}{(k+3)^{3/2}}\right]\simeq\frac{5}{2}\quad. \tag{118}$$

For at least moderately large $T\sigma$ it follows that the mean square error comes close to its minimum once

$$\frac{P}{N} > T\sigma. \tag{119}$$

If $T\sigma$ is only of the order of 10, signal to noise ratios satisfying Eq. (119) might well be encountered in practice.

Actual plots of mean square error as a function of signal to noise ratio are given in Figs. 15-17 for several combinations of parameter values. Fig. 15 uses $T\sigma = 10$, $k = 2$; in Fig. 16 $T\sigma = 100$, $k = 2$. As anticipated, the upper bound in Fig. 15 approaches its minimum near P/N = 10 db, whereas in Fig. 16 it only levels off near P/N = 20 db. Fig. 17 uses $T\sigma = 100$, $k = 10$. Comparison with Fig. 16 indicates that the effect of the k variation is relatively minor. In each case the upper bound approaches to within about 6 db of the lower bound befor it levels off at very high signal to noise ratios. At signal to noise ratios near 0 db one sees the effect of the $(N/P)^2$ terms in Eqs. (105) and (113). The region P/N < 0 db was omitted as being of limited interest.

Fig. 15

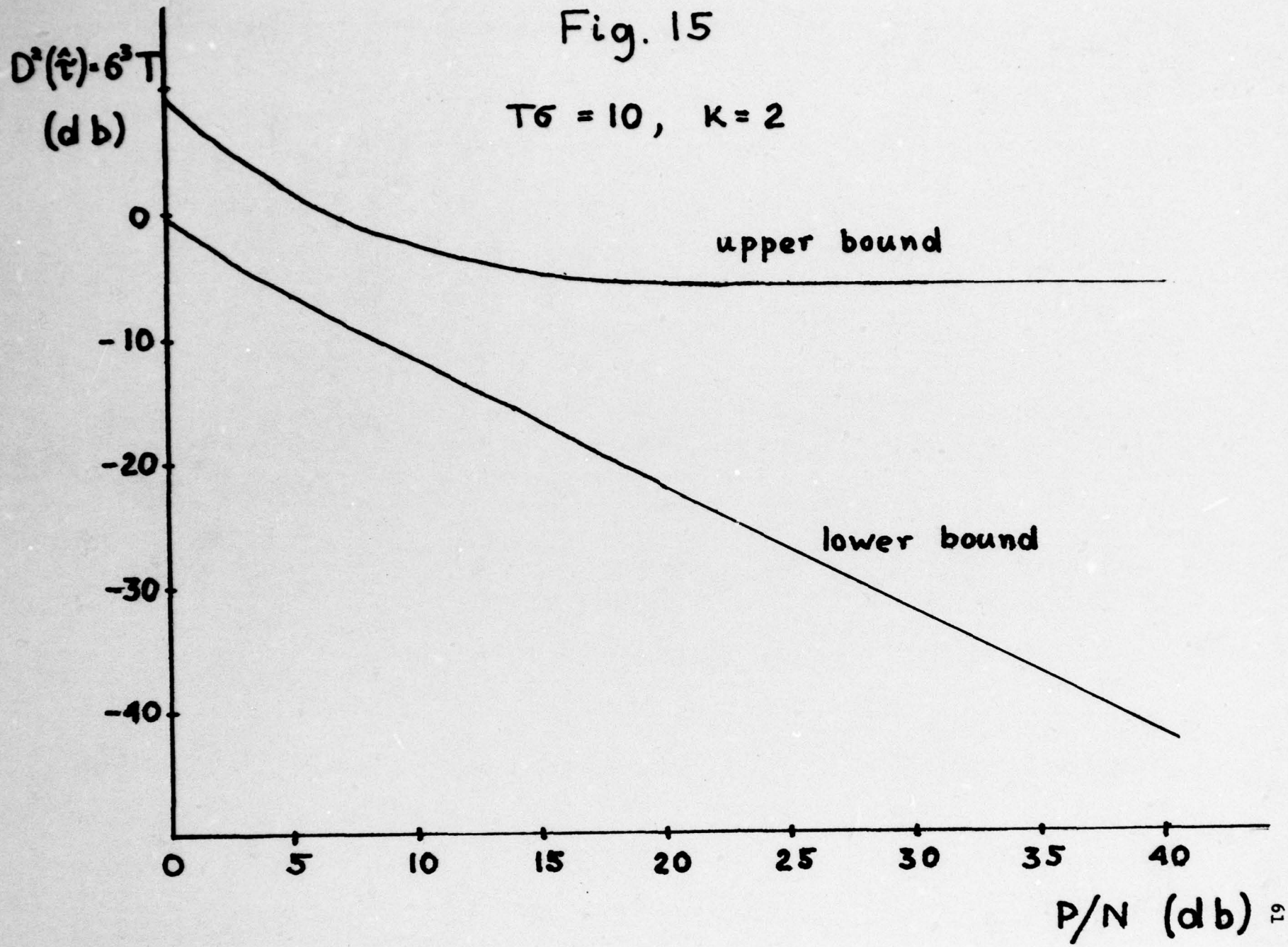
$D^2(\hat{\tau})\cdot 6^3 T$
(db)
$T\sigma = 10, \quad K = 2$
0
-10
-20
-30
-40
upper bound
lower bound
0
5
10
15
20
25
30
35
40
P/N (db)

Fig. 16

$T\sigma = 100$, $K = 2$

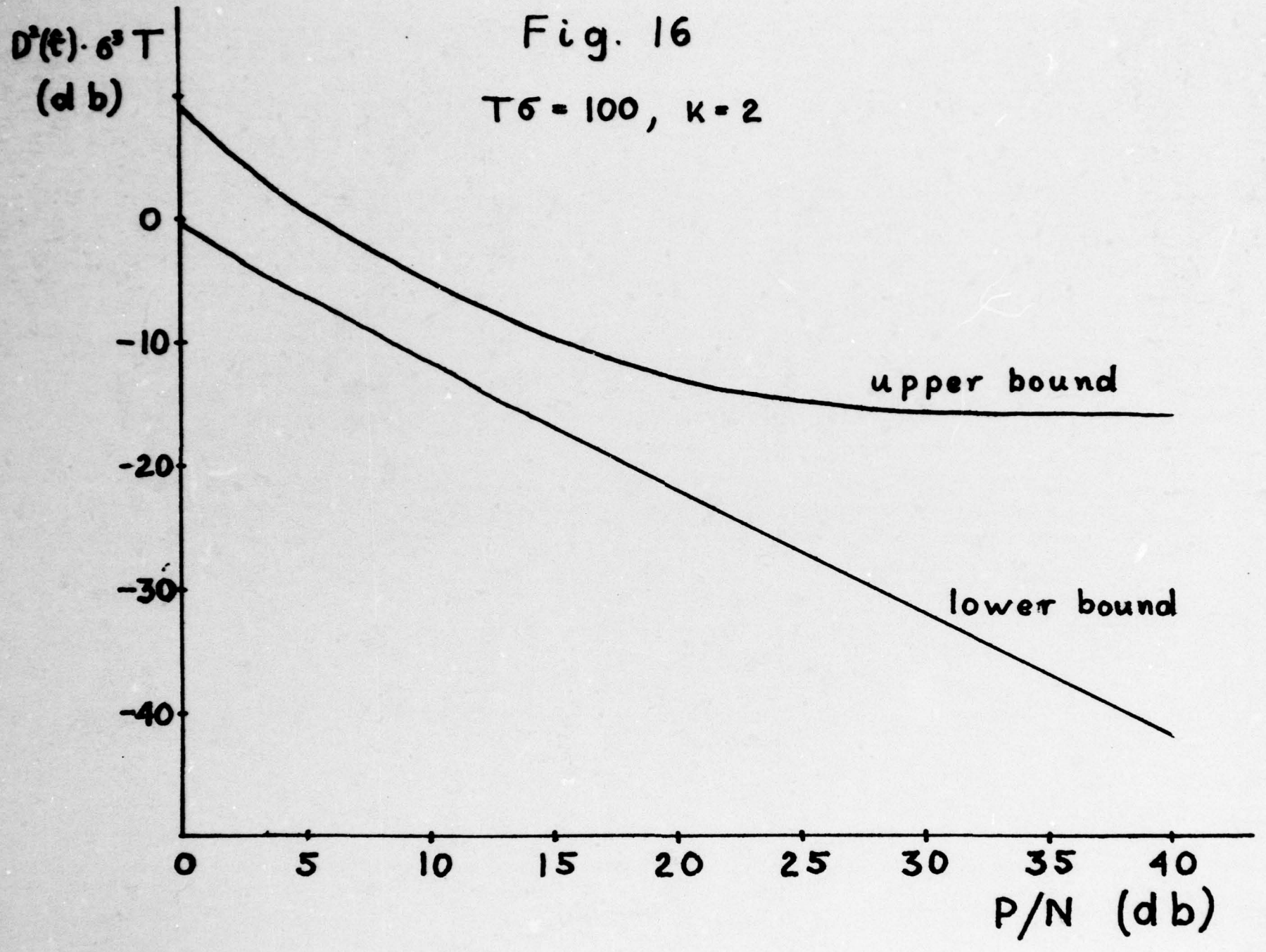

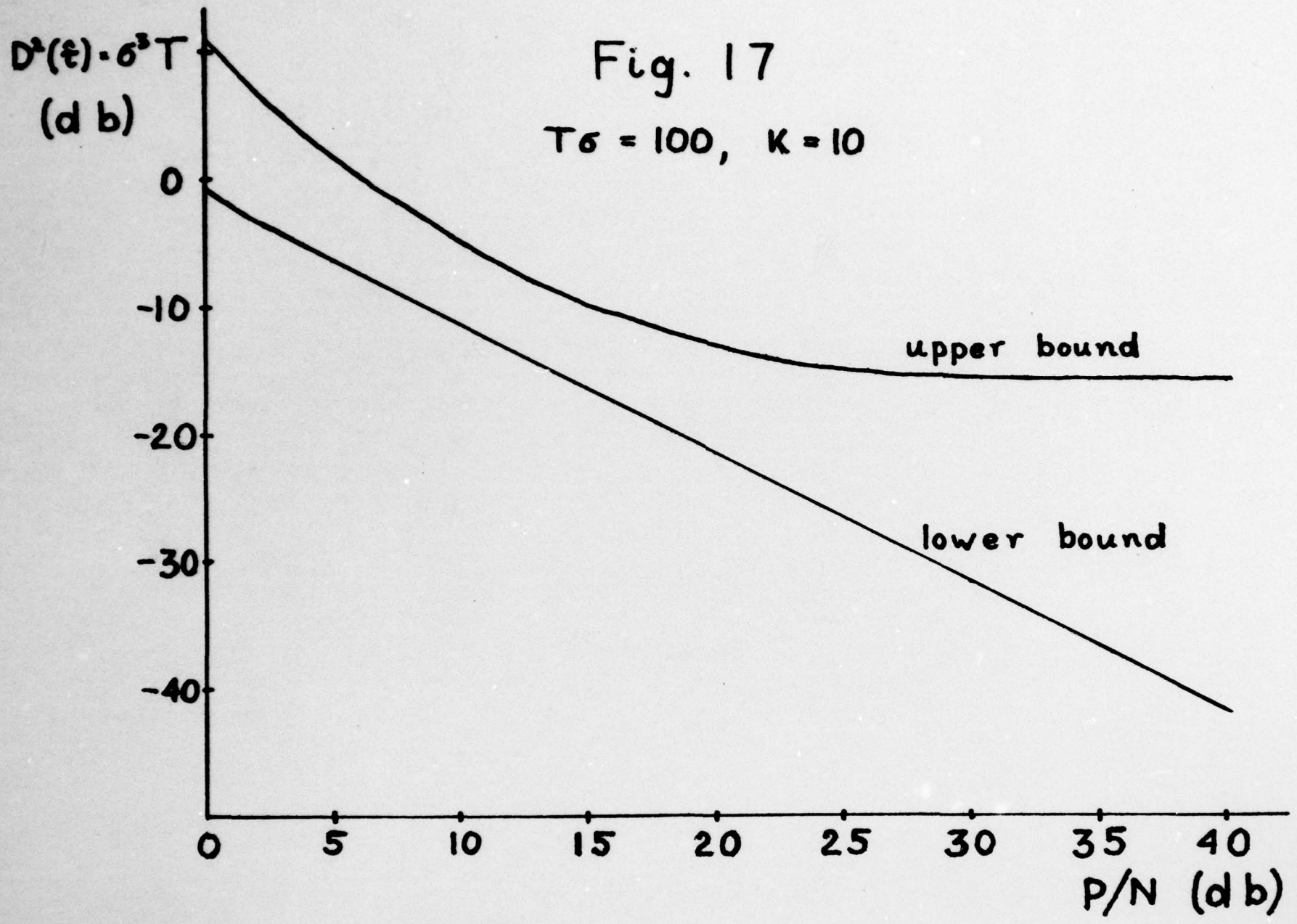
Fig. 17
Tσ = 100, K = 10
D²(t)·σ³T
(db)
0
-10
-20
-30
-40
upper bound
lower bound
0
5
10
15
20
25
30
35
40
P/N (db)

10. An Improved Envelope Tracker

In the previous section we have seen that the simple split beam envelope tracker fails to approach the theoretical optimum at every high signal to noise ratios unless the time-bandwidth product is extremely large. Since the combination of high signal to noise ratios and only moderately large time-bandwidth products is not at all unlikely in practice, we look for an improved instrumentation.

On a purely formal level, we note that the difficulty can be traced to the first (noise independent) term in Eq. (105). This component of the mean square error is derived from the first term of Eq. (102) by use of Eqs. (96) and (95). In our case the low pass filter is a simple T second integrator with the transfer function $H(\omega)$ given by Eq. (103). $|H(\omega)|^2$ decays only with the second power of frequency. As a result terms of the form $\omega^2 \exp(-a\omega^2)$ in Eq. (102) make substantial contributions to the mean square error. In particular, the noise independent term is of this form and can therefore not be ignored.

This line of reasoning immediately suggests a modification of the tracker. One need only replace the T second integrator with a low pass filter whose transfer function decays more rapidly with frequency. Computations were carried out for the low pass filter

$$H(\omega) = e^{-\frac{\omega^2}{2\sigma_0^2}} . \tag{120}$$

The frequency ratio σ/σ_0 now takes the place of the time-bandwidth product $T\sigma$. One finds that the curves of mean square error versus signal to noise ratio behave qualitatively like the upper band curves of Figs. 15-17, but that the final level is reached at a signal to noise ratio of the order $(\sigma/\sigma_0)^2$. The magnitude of the final mean square error is of order $(\sigma/\sigma_0)^{-2}$ rather than $(T\sigma)^{-1}$. A definite improvement has therefore been made.

We shall not pursue the subject of modifying the low pass filter because it is possible to take a more fundamental approach. The troublesome term in Eq. (105) describes the fluctuations produced by intermodulating signal components. When the delay $\hat{\tau}$ in Fig. 14 is adjusted properly the signal components from the two subarrays are identical and it should be possible to cancel their contribution to the output fluctuation. This idea is exploited in the instrumentation shown in Fig. 18. We shall refer to it as a balanced split beam envelope tracker.[1] It consists of 2 trackers using the same data whose outputs are subtracted. In one of the units the output of subarray 1 is differentiated, in the other that of subarray 2. The input into the integrator is therefore given by

$$y(t) = [\frac{d}{dt} R_1^2(t)]\, R_2^2(t - \hat{\tau}) - R_1^2(t)[\frac{d}{dt} R_2^2(t - \hat{\tau})]$$

$$= [\frac{d}{dt} \frac{R_1^2(t)}{R_2^2(t - \hat{\tau})}]\, R_2^4(t - \hat{\tau}). \qquad (121)$$

When there is no noise and $\hat{\tau}$ is adjusted to align the signal components, $R_1^2(t)/R_2^2(t - \hat{\tau}) = 1$ and the right side of Eq. (121) is identically equal to zero. Thus the pure signal contributions to the output fluctuation are eliminated at the operating null. There will, of course, be signal components in the error when $\hat{\tau}$ is not perfectly adjusted.

The analysis of Fig. 18 proceeds exactly as that of Fig. 14. For that reason we only state the final result

---

[1] The idea of balancing the tracker configuration and thereby removing signal contributions to the output fluctuation is equally applicable when the data vector consists of the complete sensor outputs rather than their envelopes. The usual (unbalanced) tracker is optimal only under the assumption $TW \to \infty$.

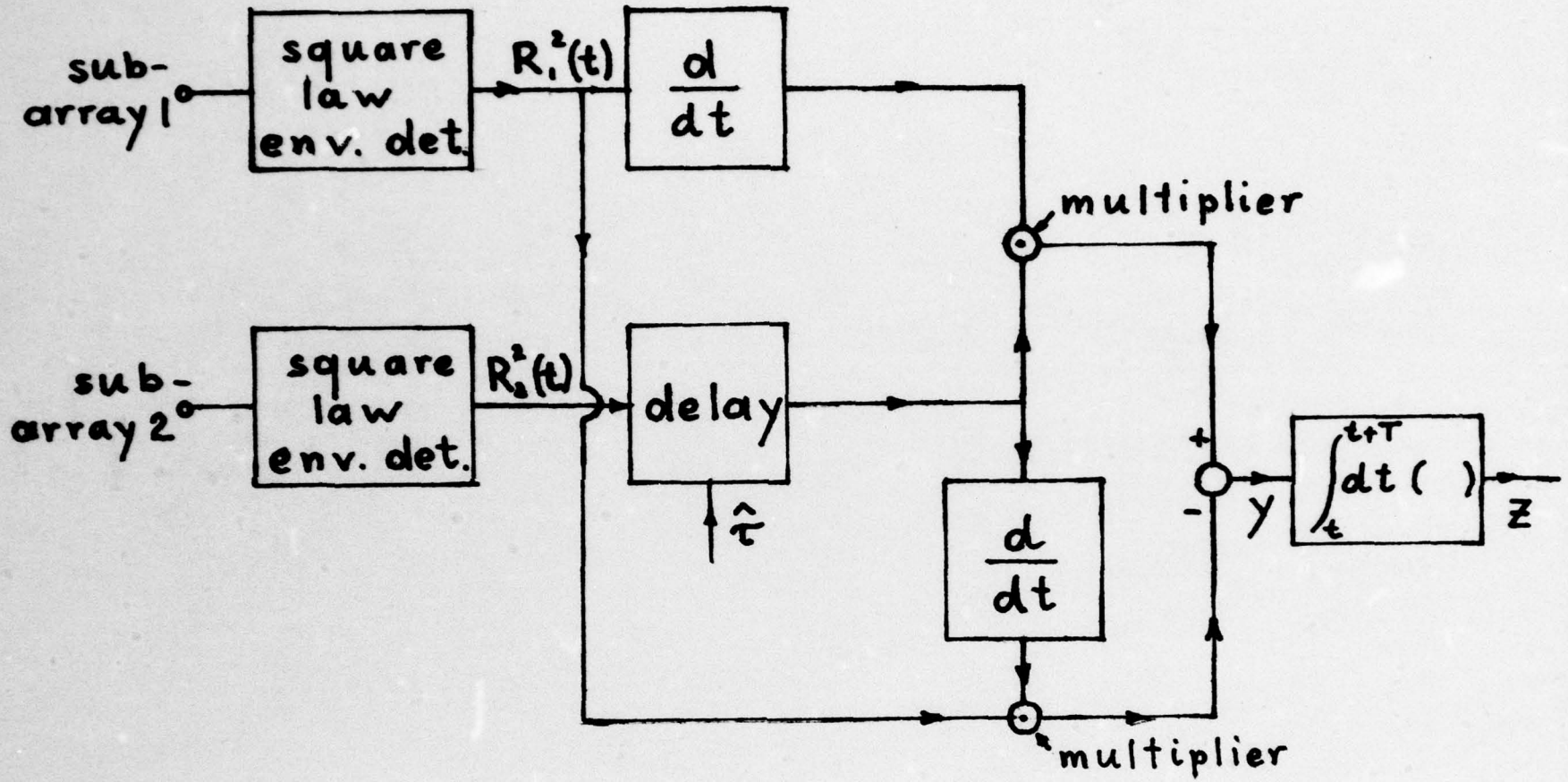
sub-
array 1
square
law
env. det.
$R_1^2(t)$
$\frac{d}{dt}$
multiplier
sub-
array 2
square
law
env. det.
$R_2^2(t)$
delay
$\hat{\tau}$
$\frac{d}{dt}$
+
-
y
$\int_t^{t+T} dt(\ )$
z
multiplier

Fig. 18

$$D^2(\hat{\tau}) =$$

$$\frac{1}{\sigma^2}\frac{1}{T\sigma}\left\{\frac{N}{P}\left[\sqrt{2\pi}\left(\frac{k}{(k+1)^{3/2}}+\frac{3k+1}{(k+3)^{3/2}}\right)+\frac{1}{T\sigma}\left(\frac{9k^2-6k+1}{4(k+1)^2}+\frac{k^2-8k-1}{(k+3)^2}\right)\right]\right.$$

$$+\left(\frac{N}{P}\right)^2\left[\sqrt{\pi}\left(\frac{\sqrt{k}}{4}+\frac{4k^2+17k+2}{8(k+1)^{3/2}}\right)+\frac{1}{T\sigma}\left(\frac{12k^2-5k+1}{8(k+1)^2}\right)\right]$$

$$\left.+\left(\frac{N}{P}\right)^3\left[\sqrt{2\pi}\,\frac{3k^2+4k}{2(3k+1)^{3/2}}+\frac{1}{T\sigma}\,\frac{13k^2+2k+3}{2(3k+1)^2}\right]+\left(\frac{N}{P}\right)^4\frac{1}{4T\sigma}\right\} \qquad (122)$$

Comparison with Eq. (105) reveals the following features:

1) Eq. (122) does not contain a noise independent term. This is, of course, the feature which motivated construction of the balanced tracker.

2) The coefficient of each power of (N/P) in Eq. (122) is smaller than the corresponding coefficient of Eq. (105). This is true for all values of k and $T\sigma$. Hence the balanced tracker is better than the conventional tracker under all operating condition.

3) For reasonably large $T\sigma$ the coefficient of the N/P term in Eq. (122) is only slightly smaller than that of the corresponding term in Eq. (105). In this important region, therefore, the balanced tracker is only marginally better than the conventional version.

A typical plot of mean square error versus signal to noise ratio for the balanced tracker is given in Fig. 19. Also shown for comparison is the lower bound and the performance curve for the conventional tracker. The parameter values are $T\sigma = 10$, $k = 2$. The curve for the balanced tracker differs from the lower bound by little more than a vertical offset of about 6 db. Potential improvements are therefore limited to an absolute maximum of 6 db. In actual fact the room for improvement is probably smaller because the lower bound is not realizable [see discussion in section 9]. The balanced split beam tracker, possibly improved by the introduction of Eckart filters, may therefore be

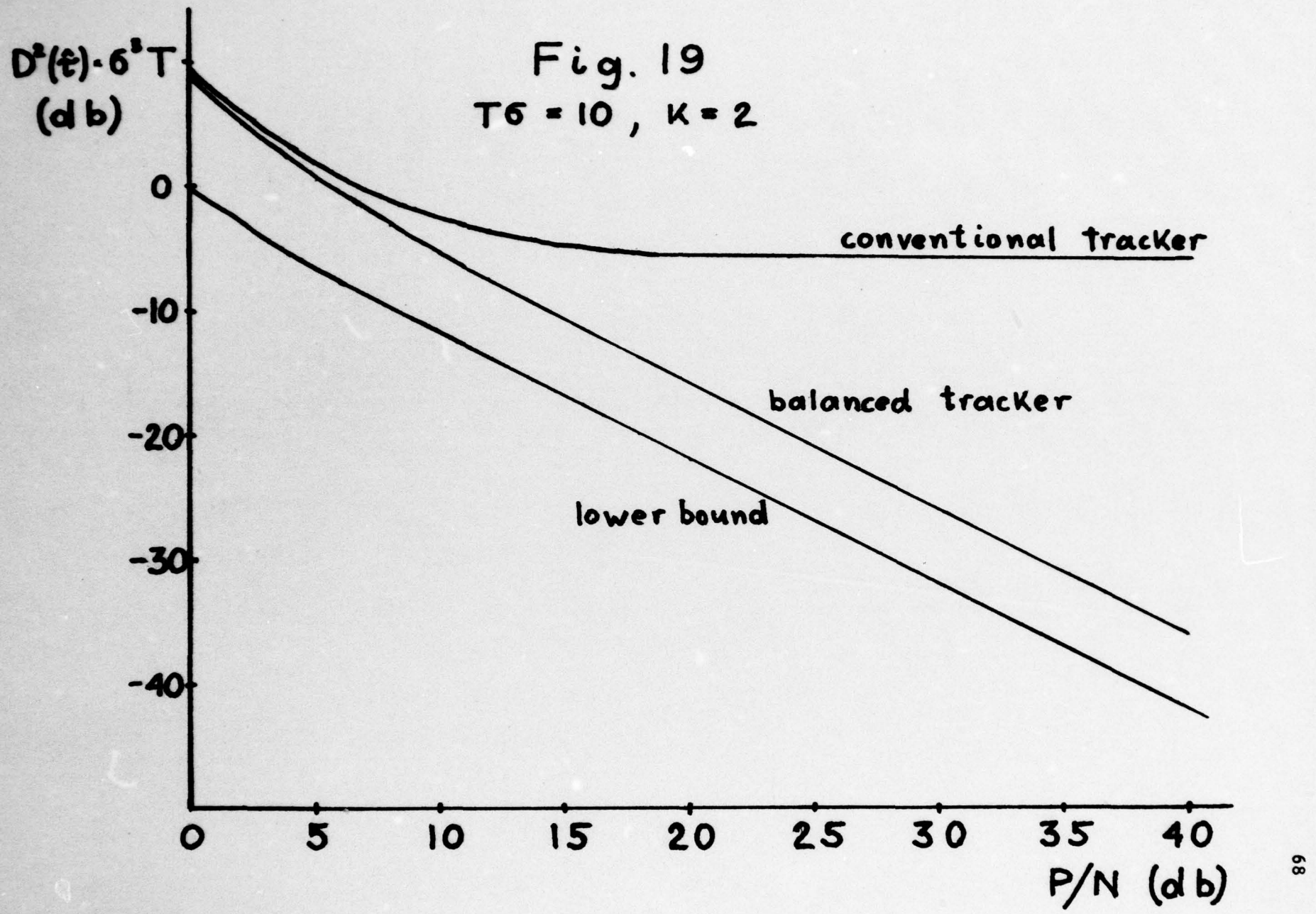
Fig. 19
T6 = 10 , K = 2
D²(t̂)·6²T
(db)
0
-10
-20
-30
-40
conventional tracker
balanced tracker
lower bound
0
5
10
15
20
25
30
35
40
P/N (db)

a very reasonable approximation to the optimum.

Further work on the balanced tracker is planned for the future. Aside from the effect of Eckart filters and similar modifications one needs to know the output fluctuation when $\hat{\tau}$ is not perfectly adjusted. Under high signal to noise ratio conditions one would expect the output fluctuations to exhibit a sharp dip near $\hat{\tau} = \tau$. This effect may actually provide a useful tool for identifying the proper value of $\hat{\tau}$.